SECOND GENERATION TRIS(2-PYRIDYL)BORATE LIGANDS: TOWARD SUPRAMOLECULAR POLYMERIC MATERIALS

by

SO YI JEONG

A thesis submitted to the

Graduate School-Newark

Rutgers, The State University of New Jersey

in partial fulfillment of the requirements

for the degree of

Master of Science

Graduate Program in Chemistry

written under the direction of

Prof. Frieder Jäkle

and approved by

_____

_____

_____

Newark, New Jersey

October, 2014

© 2014

SO YI JEONG

ALL RIGHTS RESERVED

ABSTRACT OF THE DISSERTATION

SECOND GENERATION TRIS(2-PYRIDYL)BORATE LIGANDS: TOWARD SUPRAMOLECULAR POLYMERIC MATERIALS

by SO YI JEONG

Dissertation director:

Prof. Frieder Jäkle

Supramolecular metallopolymers are generally synthesized by the self-assembly polymerization of ditopic ligands through metal-ligand binding, which is a reversible process in many cases. Supramolecular metallopolymers can provide a strong impact in polymer chemistry and materials science because of the diverse applications in self-healing, optical, electronic, and magnetic materials. The Jäkle group has recently introduced the first examples of tris(2-pyridyl)borates (Tpyb) as a new class of tridentate ligands. These new "scorpionate"-type ligands are promising because of their anticipated strong coordinating ability toward main group and transition metals, the chemical tunability, and the high stability in comparison to commonly used tris(2-pyrazolylborate)s. In addition to that, the negative charge of the tridentate ligand results

in neutral complexes with metal (II) ions, which contrasts the behavior of widely used terpyridine ligands. Based on these considerations, numerous applications in the fields of materials chemistry and catalysis are anticipated.

However, these scorpionate type ligands have not yet been studied in supramolecular chemistry. Therefore, this thesis is focused on the development of second generation tris(2-pyridyl)borate (Tpyb) ligands, where our aim is to utilize these ligands as new building blocks in the generation of supramolecular metallopolymers. The synthesis, characterization and metal complexation behavior of this new class of ligands will be discussed in this thesis. Tpyb ligands that contain additional functional groups X such as silyl and iodo groups are described. The structures of all the ligands were confirmed by multinuclear NMR spectroscopy, high-resolution MALDI mass spectrometry, and single crystal X-ray crystallography. The corresponding metal complexes $(Tpyb)_2M$ (M = Fe, Ru) were prepared and characterized by multinuclear NMR spectroscopy, and high-resolution MALDI mass spectrometry. The properties of these metal complexes were further studied by cyclic voltammetry (CV) and UV-vis spectroscopy. Finally, a fluorene-based bitopic derivate is presented as a building block for functional metal-containing polymers.

Acknowledgements

First and foremost, I would like to thank my adviser Prof. Frieder Jäkle for giving me a good opportunity to work in his group at Rutgers University. Without his constant support and guidance during every stage of my research work, all would not have been possible. I would also like to thank the current and former members of the Jäkle lab, Patrick Shipman, Fang Guo, Nurcan Baser Kirazli, Xiaodong Yin, Jiawei Chen, Wenming Wan, Gajanan Pawer, Huina Lin, Kanglei Liu, Patrycja Lupinska, Cecilia Morales, Mayyadah Yusuf, Fei Cheng, Pangkuan Chen and Mark Papadakis, for all the great moments and spending their time to help me and conversations we shared together as a group. I would especially like to thank Patrick Shipman for training and giving me supportive help in the early stages of my research. I also thank Nurcan and Fang for their warm friendship and encouragement.

This thesis is based on work supported in part by the National Science Foundation under Grant No. CHE-0956655. I would like to thank Prof. John B. Sheridan for his advice and guidance on the project. The ligand Tpyb-I was first synthesized and its single crystal X-ray structure acquired by Patrick Shipman. Patrycja Lupinska prepared the complexes Fe(Tpyb-I)$_2$ and the trimethylsilylethynyl derivative Fe(Tpyb-CCR)$_2$ as part of her undergraduate research project. I thank Prof. Roger A. Lalancette for helping me with single crystal X-ray structure determinations, Dr. Lazaros Kakalis for helping me with NMR measurements, and Dr. Roman Brukh for helping me with MALDI measurements. Also, I thank Judith Slocum, Monica Dabrowski, Lorraine McLendon, Maria Arujo and Paulo Vares for their assistance. I would also like to thank my committee members, Prof. John B. Sheridan and Prof. Roger A. Lalancette for spending their time reading my thesis, and their truly helpful feedback and advice.

Additionally, I thank all my friends, especially, So-Young Jun, Keun You, and Rami Hwang for their true friendship, encouragement and prayers. Last but not least, I would like to thank my mom, parents-in-law, and sister-in-law for their love and support. I would like to specifically thank my mom, Jong-Hwa Kim for her continuous support, love and encouragement. Finally, Chris, my beloved husband, thank you for being my life long companion and for your unconditional love.

Above all, I would like to thank God for everything.

Table of Contents

Abstract of Thesis ii

Acknowledgements iv

Table of Contents vi

List of Schemes viii

List of Figures ix

List of Tables xi

List of Abbreviations xii

Chapter A. Introduction 1

A.1 Metal-Containing Polymers 1

A.2 Supramolecular Metallopolymers 2

A.3 Scorpionate Ligands 4

A.4 1st Generation tris(2-pyridyl)borate (Tpyb) complexes 5

Chapter B. Synthesis of Second Generation Tris(2-pyridyl)borate Ligands and Their Metal Complexes 9

B.1 Introduction 9

B.2 Synthesis and Characterization of 2nd Generation Tris(2-pyridyl)borate Ligands 10

B.2.1 Synthesis of Silyl- and Iodophenyl-tris(2-pyridyl)borate Ligands 10

B.2.1.1 NMR Characterization 12

B.2.1.2 Single Crystal X-ray Diffraction Analyses 13

B.3 Synthesis and Characterization of Metal Complexes 15

B.3.1 Synthesis and Characterization of Fe(II) and Ru(II) Complexes 15

B.3.1.1 UV-visible Spectroscopy and Cyclic Voltammetry Data 18
B.4 Further Functionalization of Metal Complexes 21
B.4.1 Further Functionalization of Ru(II) Complexes 21
B.4.1.1 Introduction of Boryl Groups 21
B.4.1.2 Introduction of Alkynyl Groups 22
B.5 Development of a Bitopic Ligand 25
B.5.1 Synthesis and Characterization of the Bifunctional Ligand 3 25
B.5.1.1 NMR Characterization 27
B.5.1.2 Single Crystal X-ray Diffraction Analysis 29
B.6 Conclusions and Future Work 29
B.7. Experimental Part 30
B.7.1 Materials and General Methods 30
B.7.2 Synthetic Procedures 32
B.8 References 50
Appendix 52
VITA 54

List of Schemes

Scheme A1. Synthesis of Fe(II) complexes. 7

Scheme A2. Nitroxide-mediated polymerization of StTpyb and chain extension with styrene. 8

Scheme B1. Synthesis of ligands Tpyb-Si (X = $SiMe_3$) and Tpyb-I (X = I) in CH_2Cl_2; the magnesium complexes were found as products in small amounts. 11

Scheme B2. Synthesis of Fe(Tpyb-X)$_2$ complexes. (X = $SiMe_3$ or I) 16

Scheme B3. Synthesis of Ru(Tpyb-X)$_2$ complexes. (X = $SiMe_3$ or I) 17

Scheme B4. Attempted further functionalization of metal complexes by introduction of boryl groups. 22

Scheme B5. Further functionalization of metal complexes by introduction of alkynyl groups. 23

Scheme B6. Proposed synthesis of metallo-supramolecular polymeric materials by cross-coupling reactions. 23

Scheme B7. Synthesis of bifunctional ligand 3 ($Tpyb_2$-FL) (PC = propylene carbonate). 26

Scheme B8. Attempted synthesis of metallo-supramolecular polymeric materials upon complexation of bifunctional ligand 3 ($Tpyb_2$-FL). 26

List of Figures

Figure A1. Schematic illustrations of the metallo-supramolecular polymerization of ditopic ligands with transition and lanthanide metal ions. 3

Figure A2. Schematic representation of the structures of typical N-based tridentate ligands in supramolecular polymer chemistry. 3

Figure A3. Schematic representation of tris(pyrazolyl)borate (Tp) derivatives. 5

Figure A4. Representation of a first generation tris(2-pyridyl)borate ligand. 6

Figure A5. Ball and stick view of the extended structure of $Fe(Tpyb\text{-}R)_2$ (R = t-butyl; crystallized from cyclohexane) along the crystallographic c-axis. 7

Figure B1. Schematic representation of targeted 2nd generation tris(2-pyridyl)borate ligands. 9

Figure B2. Numbering scheme of the pyridine and phenyl rings. 12

Figure B3. Comparison of ^{1}H NMR spectra of silyl ligand 1 (Tpyb-Si) and iodo ligand 2 (Tpyb-I) in $CDCl_3$ (Py-NH not shown). 13

Figure B4. Overlay of ^{11}B NMR spectra of silyl ligand 1 (Tpyb-Si) and iodo ligand 2 (Tpyb-I) in $CDCl_3$. 13

Figure B5. Ball and stick representations of the X-ray structures of (a) silyl ligand 1 (Tpyb-Si) and (b) iodo ligand 2 (Tpyb-I). Hydrogen atoms are omitted for clarity except for the acidic proton H1. 14

Figure B6. Ball and stick representation of the X-ray structure of the $Mg(Tpyb\text{-}Si)_2$. Hydrogen atoms and solvent molecules are omitted for clarity. 15

Figure B7. Overlay of ^{11}B NMR spectra of ligand 1 (Tpyb-Si), the $Fe(Tpyb\text{-}Si)_2$ and $Ru(Tpyb\text{-}Si)_2$ complexes in C_6D_6. 17

Figure B8. Comparison of the ^{1}H NMR spectra (aromatic region) of ligand 1 (Tpyb-Si), the $Fe(Tpyb\text{-}Si)_2$ and $Ru(Tpyb\text{-}Si)_2$ complexes in C_6D_6. 18

Figure B9. (a) Comparison of UV-vis spectra of $Fe(Tpyb\text{-}Si)_2$ and $Ru(Tpyb\text{-}Si)_2$ in CH_2Cl_2. (b) Corresponding photographs (left (orange): $Fe(Tpyb\text{-}Si)_2$, λ_{max} = 485 nm; right (yellow): $Ru(Tpyb\text{-}Si)_2$; λ_{max} = 441 nm). 19

Figure B10. Comparison of cyclic voltammograms of (a) $Fe(Tpyb\text{-}Si)_2$ and (b) $Ru(Tpyb\text{-}Si)_2$. 1×10^{-3}M with 0.1M $[Bu_4N]PF_6$ in CH_2Cl_2 as the supporting electrolyte (scan rate 100mV/s; Ag/AgCl was used as reference and set as zero). 20

Figure B11. Overlay of ^{1}H NMR spectra (aromatic region) of $Fe(Tpyb\text{-}CCR)_2$ and $Ru(Tpyb\text{-}CCR)_2$ in THF-d_8. 24

Figure B12. Overlay of ^{13}C NMR spectra (aromatic and alkynyl region) of $Fe(Tpyb\text{-}CCR)_2$ and $Ru(Tpyb\text{-}CCR)_2$ in THF-d_8. 24

Figure B13. Numbering scheme of the pyridine and fluorene rings. 27

Figure B14. ^{1}H NMR spectrum (aromatic region) of $Tpyb_2$-FL in $CDCl_3$. 28

Figure B15. ^{11}B NMR spectrum of $Tpyb_2$-FL in $CDCl_3$. 28

Figure B16. Ball and stick representation of the X-ray structure of $Tpyb_2$-FL. Hydrogen atoms are omitted for clarity except for the acidic protons H1. 29

List of Tables

Table B1. Summary of UV-vis absorption and CV data. 21

List of Abbreviations

CT	charge transfer
CV	cyclic voltammetry
NMR	nuclear magnetic resonance
Ph	phenyl
Py	pyridine
THF	tetrahydrofuran
PC	propylene carbonate
UV-vis	Ultraviolet-visible
MALDI	matrix-assisted laser desorption ionization
DCM	dichloromethane
Tpyb	tris(2-pyridyl)borate
Tp	tris(pyrazolyl)borate

CHAPTER A. Introduction

A.1 Metal-Containing Polymers

Over the past decade, metal-containing polymers or metallopolymers have attracted interest because of their numerous applications in the field of materials chemistry and polymer science [1]. A great advantage of the presence of transition metal atoms in polymer chains is that the electrochemical, catalytic, optical, redox, and magnetic properties of metal complexes are combined with the properties of organic materials [2]. Therefore, the basic physical and chemical properties of metals play an important role in new functional materials. Besides their potential use as construction materials, self-assembled functional metal-containing polymeric materials are promising for the development of new electronic, optical, biological and energy-related materials [3].

Polymeric materials offer many advantages and are widely used as building blocks for new functional materials [2-3]. However, there are disadvantages associated with polymeric materials that are not shared by metals. In comparison to metals, they have relatively low thermal stability and lower mechanical strength [2-3]. Therefore, the idea of combining metal elements with synthetic polymeric materials into metal-containing polymers offers many advantages and minimizes their disadvantages [2-3]. For example, main chain conjugated metallopolymers are an interesting class of materials with desirable mechanical and electronic properties [2]. The incorporation of transition metal atoms into pi-conjugated polymers offers an attractive base for further tuning the physical properties; they have become a prominent class of metal-organic hybrid materials [4]. Moreover, the self-assembly of functional monomers into metal-containing polymeric

materials through the utilization of non-covalent bonds has proven very useful in supramolecular chemistry [4].

A.2 Supramolecular Metallopolymers

Supramolecular polymers have been widely studied with respect to their interesting electronic, optical and mechanical properties over the past several years [4]. Supramolecular assembly can occur through weak interactions (non-covalent intermolecular interactions), such as metal coordination, hydrogen bonding, pi-pi interactions, etc. Metal coordination typically introduces strong and robust supramolecular structures through metal-ligand bonds [4]. Metal-ligand interactions can be used to prepare linear supramolecular polymeric materials, but the use of metal ions that bind 3 ligands can also result in branching/cross linking (Figure A1) [5]. In general, the formation of supramolecular metallopolymers is a self-assembly process of ditopic ligands through metal-ligand binding and as such occurs spontaneously without an initiator [6]. The strength of the coordinate M-L bonds depends on both the nature of the metal ion and ligand used; in many cases the assembly process is reversible, which implies that external stimuli can result in changes in the characteristics of the materials [7]. This behavior may be beneficial in applications related to optical, electronic, and interesting magnetic materials, etc [8]. The class of supramolecular metallopolymers is also promising in the application of self-healing materials. Again, the reversible nature of the metal-ligand interaction, the increased strength with respect to other supramolecular chemistry interactions such as hydrogen bonding and the response of metal complexes to external stimuli result in unique materials are beneficial [10]. Typical N-based tridentate

ligands in supramolecular polymer chemistry are terpyridines used by the Schubert group, bis(pyrazolyl)pyridines by the Ruben group, and bis(methylbenziimidazolyl)pyridines by the Rowan and Weder groups (Figure A2) [7,9].

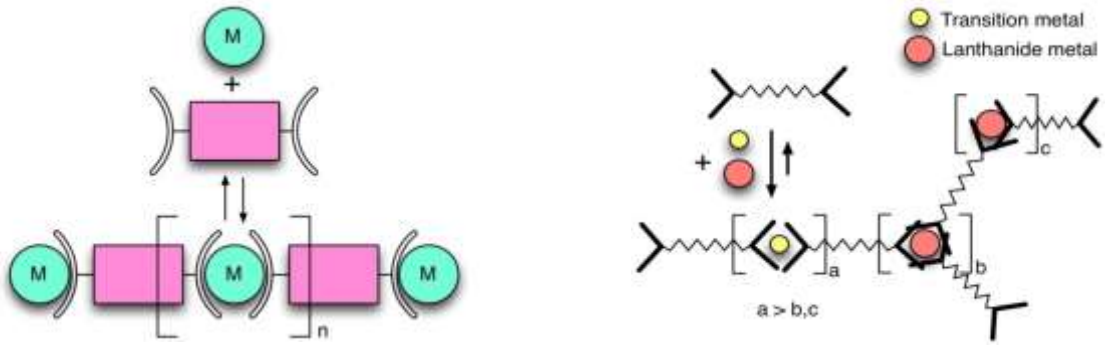

Figure A1. Schematic illustrations of the metallo-supramolecular polymerization of ditopic ligands with transition and lanthanide metal ions. Adopted from *Macromolecules* 2005, 39, 651-657; *Macromolecules* 2006, 39, 4069-4075.

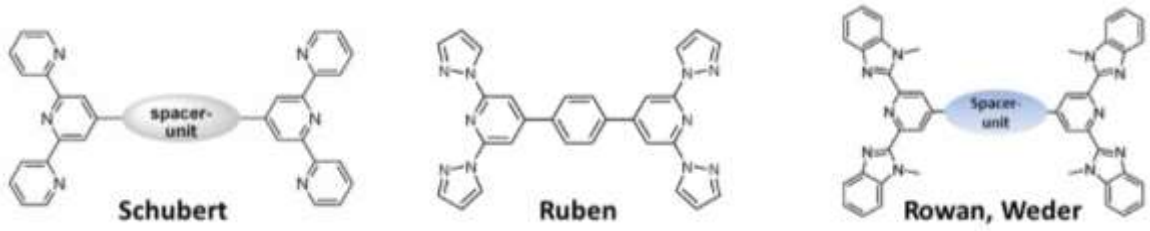

Figure A2. Schematic representation of the structures of typical N-based tridentate ligands in supramolecular polymer chemistry. Adopted from *Macromolecules* 2006, 39, 4069-4075; *Macromolecules* 2008, 41, 2157-2163; *Chem. Soc. Rev.*, 2011, 40, 1459-1511.

A.3 Scorpionate Ligands

Besides the ligands displayed in Figure A2, we are interested in utilizing scorpionate ligands because there are significant differences to be expected in terms of their properties and metal complex geometries and also these scorpionate type ligands have not yet been studied in supramolecular chemistry. The most well known "scorpionate"-type ligands are the tris(pyrazolyl)borates (Tp) ligands (Figure A3) first introduced by Trofimenko in 1966 [11] [12]. They have been widely used in the fields of catalysis and materials chemistry and are highly useful ligands in coordination chemistry because of their tunability and strong binding to most metals in the periodic table [13]. The second generation of Tp ligands, which features substituents on the pyrazolyl groups that are introduced for steric and electronic-fine tuning, was followed by a third generation Tp ligands, in which functional groups on the terminal substituent on boron make for even greater tunability and diversity [14] [15] [12]. We also note that more recently the Wagner group introduced redox active ferrocene-based Tp derivatives as well [16]. Even though pyrazolylborate ligands have many advantages, there have been concerns about the stability of the B-N bonds. Decomposition of Tp ligands with formation of the parent pyrazoles is often observed and can be catalyzed by Bronsted acids or Lewis acids. Based upon these considerations, the Jäkle group has recently introduced a first generation of tris(2-pyridyl)borates (Tpyb) as a new class of tridentate scorpionate-type ligands [12, 17].

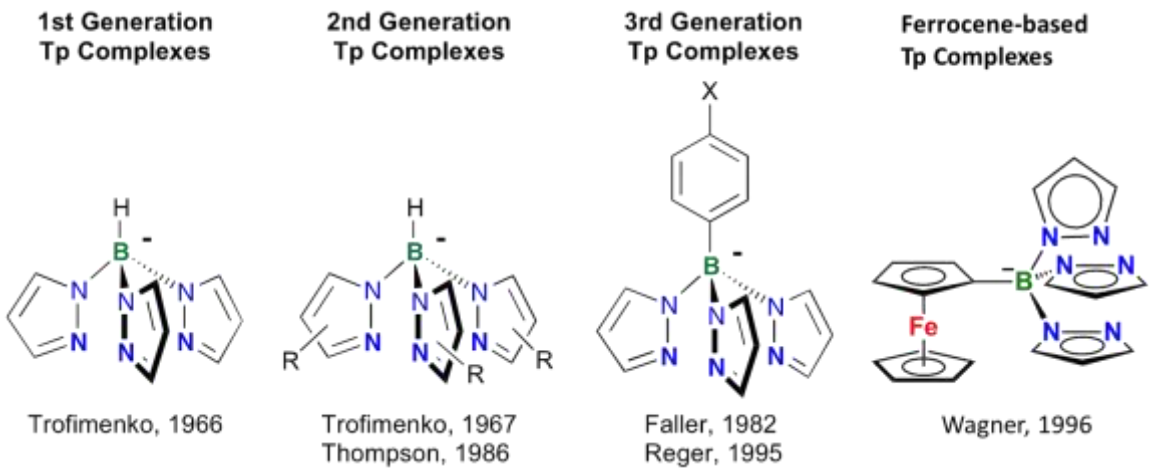

Figure A3. Schematic representation of tris(pyrazolyl)borate (Tp) derivatives. Adopted from *Inorg. Chem.* 2013, *52*, 9440-9447; *Inorg. Chem.* 1997, *36*, 2103-2111.

A.4 1st Generation tris(2-pyridyl)borate (Tpyb) complexes

Tris(2-pyridyl)borates (Tpyb) (Figure A4) serve as a new class of tridentate scorpionate-type ligands, in which the pyrazolyl groups are replaced with pyridyl groups [17]. Boron forms strong and significantly less polar bonds to carbon, thereby providing better stability. In addition to an enhanced stability, these "scorpionate'-type ligands are promising because of their proven strong coordinating ability toward transition metals and the chemical tunability [17]. Initially, the Jäkle group studied the ligand properties and ability of tris(pyridyl)borate derivatives to form metal complexes with Fe(II) ions (Scheme A1). As an example, treatment of tris(2-pyridyl)borate ligand with $FeCl_2$ in THF/MeOH in the presence of triethylamine resulted in a red solid that was purified by column chromatography and recrystallized from toluene [17]. In the crystal structure the Fe atom sits on an inversion center and the complex adopts a slightly distorted octahedral

geometry as a result of a tridentate facial coordination mode. The extended structure of the Fe complex prepared from toluene or cyclohexane solution displays large hexagonal channels that are formed by non-covalent assembly. The solvent could be removed under high vacuum without decomposition. Therefore, the cavities could be utilized to capture and store gases and possibly other small molecule (Figure A5) [12].

Jäkle and Sheridan have also demonstrated the synthesis of a new polymerizable scorpionate ligand based on a tris(2-pyridyl)borate derivative (Scheme A2). Controlled nitroxide-mediated polymerization of a styryl derivative led to successful formation of homo- and block copolymers [18]. The block copolymer product undergoes self-assembly in selective solvents and can be complexed with transition metal ions.

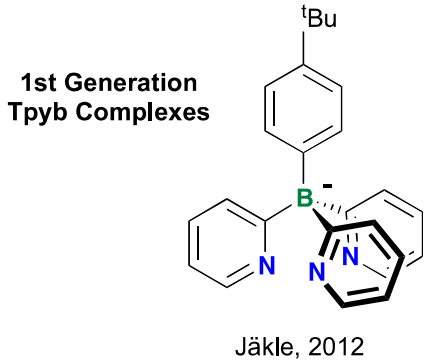

Figure A4. Representation of a first generation tris(2-pyridyl)borate ligand. Reproduced from *Inorg. Chem.* 2013, *52*, 9440-9447.

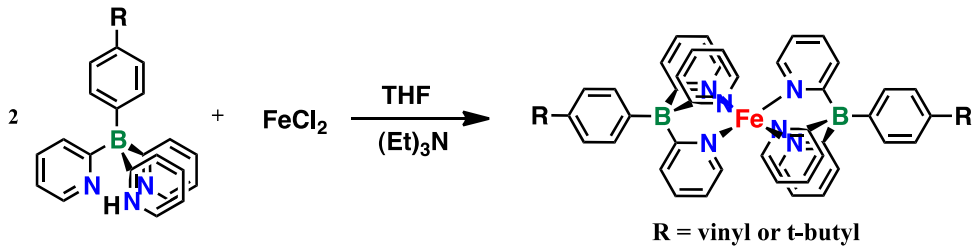

Scheme A1. Synthesis of Fe(II) complexes. Reproduced from *Inorg. Chem.* 2013, *52*, 9440-9447.

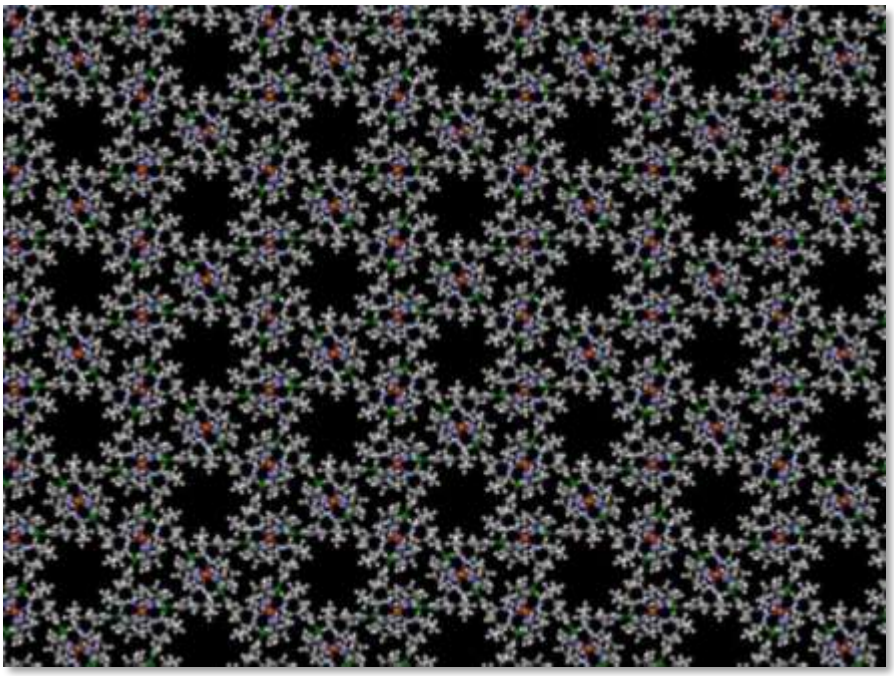

Figure A5. Ball-and stick view of the extended structure of Fe(Tpyb-R)$_2$ (R= t-butyl; crystallized from cyclohexane) along the crystallographic c-axis. Reproduced from *Inorg. Chem.* 2013, *52*, 9440-9447.

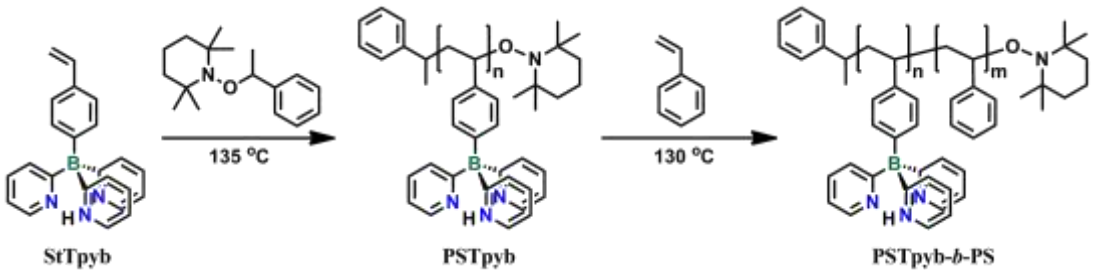

Scheme A2. Nitroxide-mediated polymerization of StTpyb and chain extension with styrene. Reproduced from ACS Macro Letters 2013, 2, 1056-1060.

CHAPTER B. Synthesis of Second Generation Tris(2-pyridyl)borate Ligands and Their Metal Complexes

B.1 Introduction

Based on the unique aspects and favorable properties of 1st generation Tpyb ligands, described in Chapter A, this thesis is focused on the development of 2nd generation Tpyb ligands (Figure B1) to create new functional materials and to introduce these more robust Tpyb ligands as new versatile building blocks in supramolecular polymer chemistry.

Our approach to the 2nd generation of tris(2-pyridyl)borates is to introduce additional functional groups X such as iodo, silyl, boryl, or alkynyl groups that could be used for coupling reactions to generate polymeric materials. Moreover, a fluorene-based bitopic derivate is presented that may serve as building block for functional metal-containing polymers. We anticipate broad applications of this new ligand class in the field of catalysis, materials and supramolecular polymer chemistry. The synthesis, characterization and metal complexation behavior are described in the following.

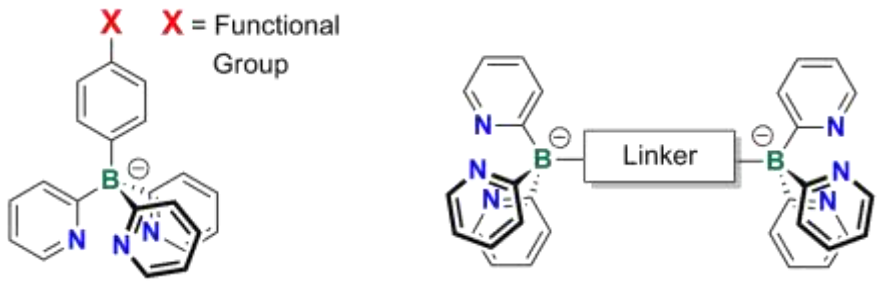

Figure B1. Schematic representation of targeted 2nd generation tris(2-pyridyl)borate ligands.

B.2 Synthesis and Characterization of 2nd Generation Tris(2-pyridyl)borate Ligands

The synthesis of 2nd generation tris(2-pyridyl)borate ligands is described in the following. As previously reported [17], the major synthetic breakthrough was the adoption of a 2-pyridyl Grignard reagent that was prepared by reaction of isopropyl magnesium chloride with 2-bromopyridine.

B.2.1 Synthesis of Silyl- and Iodophenyl-tris(2-pyridyl)borate Ligands

4-Trimethylsilylphenyl dibromoborane and 4-iodophenyl dibromoborane were selected as the precursors and prepared as previously reported [19]. 1,4-Bis(trimethylsilyl)benzene was reacted with boron tribromide in dichloromethane and the volatile materials were evaporated under high vacuum to give the product as a light green liquid. Similarly, 4-iodophenyl dibromoborane was prepared from reaction between 1-iodo-4-trimethylsilylbenzene and boron tribromide in dichloromethane and obtained as a light brown liquid.

The synthesis of the corresponding 2nd generation tris(2-pyridyl)borate ligands (Scheme B1) was achieved by addition of a dichloromethane solution of 4-trimethylsilylphenyl dibromoborane or 4-iodophenyl dibromoborane to a dichloromethane solution of the Grignard 2-PyMgCl. Drop-wise addition of the solution of the borane to the pyridyl Grignard reagent solution is important to maintain an excess amount of pyridyl Grignard reagent throughout the reaction, which helps reduce the side reactions between dibromoborane and THF [17]. An aqueous solution of $NaHCO_3$ was then used to quench the reaction and the product was extracted into dichloromethane. The dichloromethane

solution was brought to dryness by rotary evaporation and the product was extracted into methanol (silyl derivative) or acetone (iodo derivative). Finally the trimethylsilylphenyl-tris(2-pyridyl)borate free acid (Tpyb-Si) and iodophenyl-tris(2-pyridyl)borate free acid (Tpyb-I) were purified by column chromatography on alumina gel. It is worth noting that a small amount of methanol-insoluble material was found to contain another borate species, which showed a characteristic sharp peak in the ^{11}B NMR spectrum. Recrystallization from cyclohexane afforded colorless crystals, which were identified by single crystal X-ray diffraction to be the bis-coordinated Mg(Tpyb-Si)$_2$ complex.

When a similar reaction was carried out in toluene, the reaction solution showed a larger amount of the bis-coordinated magnesium complex. The toluene solvent was removed completely and extracted from methanol to give a white solid residue. Both the pyridylborate free acid and the magnesium halide salts were extracted into methanol solution leaving behind the complex Mg(Tpyb-Si)$_2$ in high purity. This method allowed for isolation of the Mg complex in higher yield.

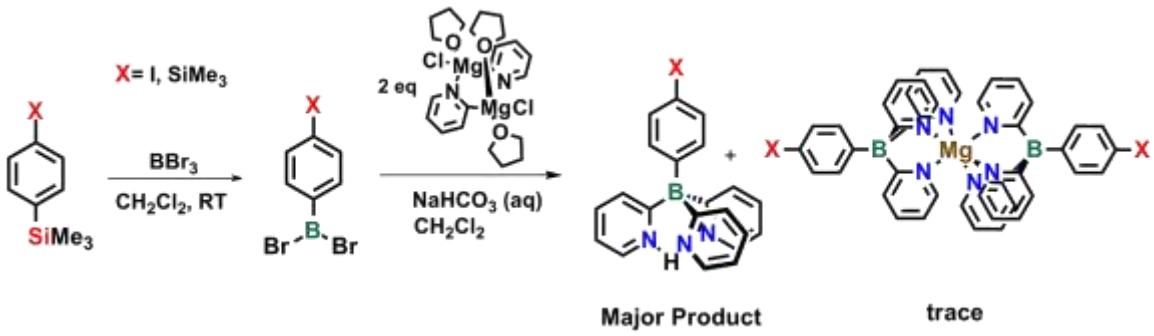

Scheme B1. Synthesis of ligands Tpyb-Si (X = SiMe$_3$) and Tpyb-I (X = I) in CH_2Cl_2; the magnesium complexes were found as side products in small amounts.

B.2.1.1 NMR Characterization

The silyl ligand 1 (Tpyb-Si) and iodo ligand 2 (Tpyb-I) were analyzed by multinuclear NMR and the assignments of the protons in the pyridine and phenyl rings are depicted in Figure B2. The ^{1}H NMR spectra of Tpyb-Si and Tpyb-I in $CDCl_3$ feature the expected patterns for pyridyl and phenyl rings, as well as the appearance of a singlet at 0.21ppm, that confirms the presence of the silyl group of Tpyb-Si (Figure B3). Singlets at 18.7 ppm and 16.6 ppm confirm the presence of a nitrogen-bound proton (not shown). The ^{11}B NMR spectra of both compounds showed a sharp singlet near -10 ppm, which is in the region expected for tetraarylborates (Figure B4). The ^{13}C NMR spectra exhibited quartets near 184 ppm and 157 ppm, which are due to coupling of boron to the boron-bound pyridyl carbon atoms and phenyl carbon atoms, respectively.

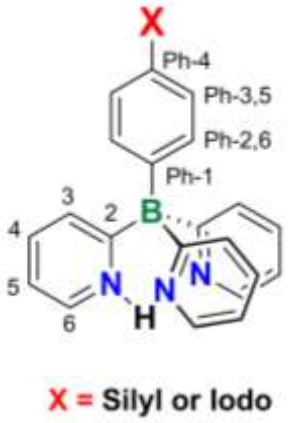

Figure B2. Numbering scheme of the pyridine and phenyl rings.

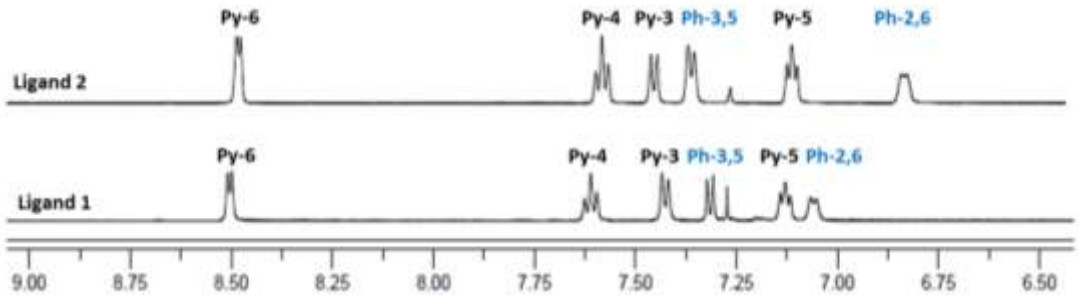

Figure B3. Comparison of ^{1}H NMR spectra of silyl ligand 1 (Tpyb-Si) and iodo ligand 2 (Tpyb-I) in $CDCl_3$ (Py-NH not shown). (Assignments based on comparison to literature data; Chem. Commun. 2012, *48*, 6930-6932.)

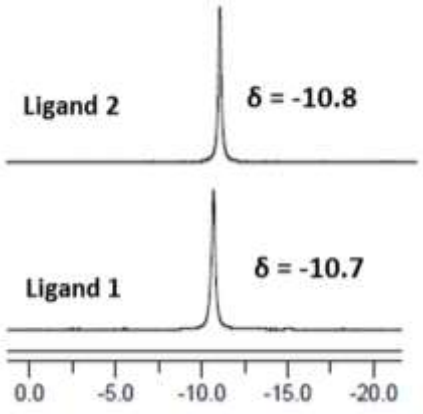

Figure B4. Overlay of ^{11}B NMR spectra of silyl ligand 1 (Tpyb-Si) and iodo ligand 2 (Tpyb-I) in $CDCl_3$.

B.2.1.2 Single Crystal X-ray Diffraction Analyses

The structures of the ligands were further confirmed by single-crystal X-ray diffraction analysis. Single crystals for X-ray diffraction analysis of the tridentate ligands were

obtained by slow solvent evaporation of a solution in a mixture of toluene and hexanes (Tpyb-Si) or DCM and hexanes (Tpyb-I). Based on the single-crystal X-ray data one independent molecule was found in the unit cell of silyl ligand 1 (Tpyb-Si) and iodo ligand 2 (Tpyb-I). The presence of a nitrogen-bound proton was confirmed (Figure B5). The B-C distances to the phenyl ring (1.637(3), 1.635(4) Å) are similar to those of the pyridyl substituents (1.625(3) to 1.639(3) Å, 1.635(4) to 1.639(4) Å), and the C-B-C angles (107.26(17) to 111.37(17)^{o}, 106.7(2) to 110.6(2)^{o}) are in the range typically observed for arylborates. This confirms the absence of any significant steric strain.

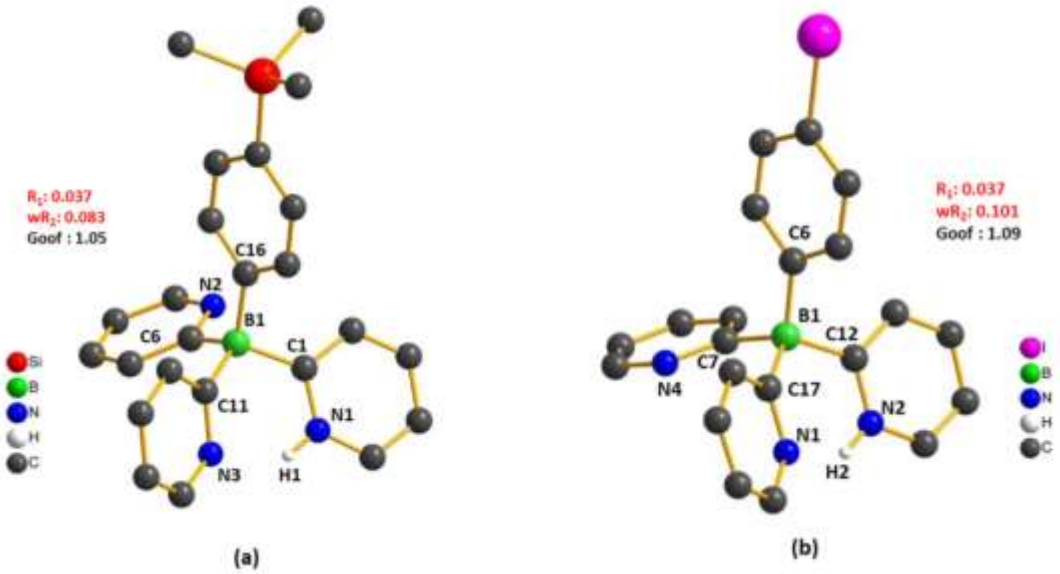

Figure B5. Ball-and stick representations of the X-ray structures of (a) silyl ligand 1 (Tpyb-Si) and (b) iodo ligand 2 (Tpyb-I). Hydrogen atoms are omitted for clarity except for the acidic proton H1 (or H2).

Single crystals of Mg(Tpyb-Si)$_2$ for X-ray diffraction analysis were obtained by slow evaporation of a solution in cyclohexane. Three main molecules and five cyclohexane

solvent molecules were found in the unit cell (Figure B6). The Tpyb-Si moieties act as tridentate ligands in the bis-coordinated magnesium complex. The Mg atom sits on an inversion center and the complex adopts a slightly distorted octahedral geometry. Based on the X-ray data two of the Mg-N bonds are similar in length (2.188(3), 2.198(3) Å), but the third is relatively shorter (2.147(3) Å).

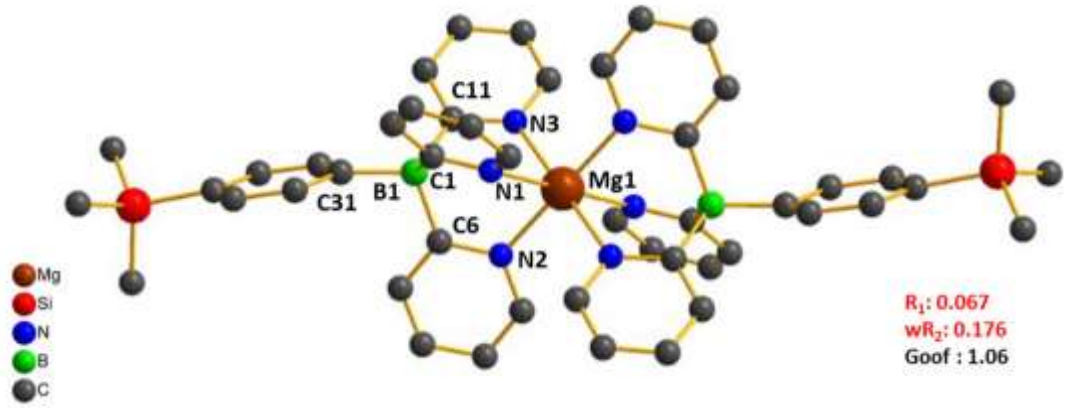

Figure B6. Ball and stick representation of the X-ray structure of Mg(Tpyb-Si)$_2$. Hydrogen atoms and solvent molecules are omitted for clarity.

B.3 Synthesis and Characterization of Metal Complexes

B.3.1 Synthesis and Characterization of Fe(II) & Ru(II) Complexes

The respective tris(2-pyridyl)borate ligand (Scheme B1) was reacted with $FeCl_2$ in tetrahydrofuran in the presence of triethylamine to give the corresponding Fe(II) complex (Scheme B2) as a red solid that was purified by column chromatography with a 1:9 mixture of tetrahydrofuran and hexanes as the eluent. Treatment of the respective ligand (Scheme B1) with a solution of $RuCl_2(DMSO)_4$ in ethanol in the presence of triethylamine gave the corresponding Ru(II) complex (Scheme B3) as a yellow/green

solid that was collected by filtration of the hot suspension and washed with acetone and ether. The products were studied by ^{11}B and ^{1}H NMR analysis. While the ^{11}B NMR shifts of ligand 1 (Tpyb-Si), Fe(Tpyb-Si)$_2$ and Ru(Tpyb-Si)$_2$ are similar (Figure B7), the pattern of the pyridyl rings in the ^{1}H NMR spectra is changed. An overlay of the ^{1}H NMR spectra of ligand 1 (Tpyb-Si) and the Fe(Tpyb-Si)$_2$ and Ru(Tpyb-Si)$_2$ complexes is shown in Figure B8. As a result of the mutual shielding effects, the pyridyl proton 6 that is near the central Fe(II) and Ru(II) ions exhibited a large upfield shift. Simultaneously, the aromatic protons were shifted downfield upon metal complexation. Similar patterns were also observed for ligand 2 (Tpyb-I) and the corresponding complexes Fe(Tpyb-I)$_2$ and Ru(Tpyb-I)$_2$. We note that the Fe(II) complexes tend to get easily oxidized to the Fe(III) species in chlorinated solvents. They tend to show better stability in benzene, but the solubility is not as good as in THF as the preferred NMR solvent. The Ru(II) complexes are more stable than the Fe(II) complexes even under air, but the data were also acquired in benzene (or THF) as the NMR solvent in order to allow for comparison.

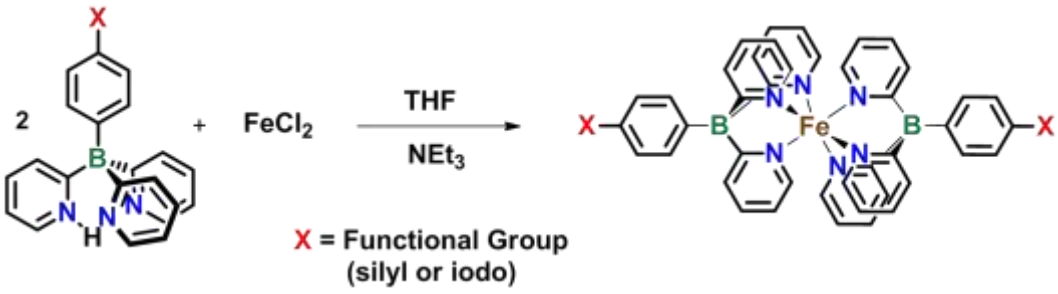

Scheme B2. Synthesis of Fe(Tpyb-X)$_2$ complexes. (X = SiMe$_3$ or I)

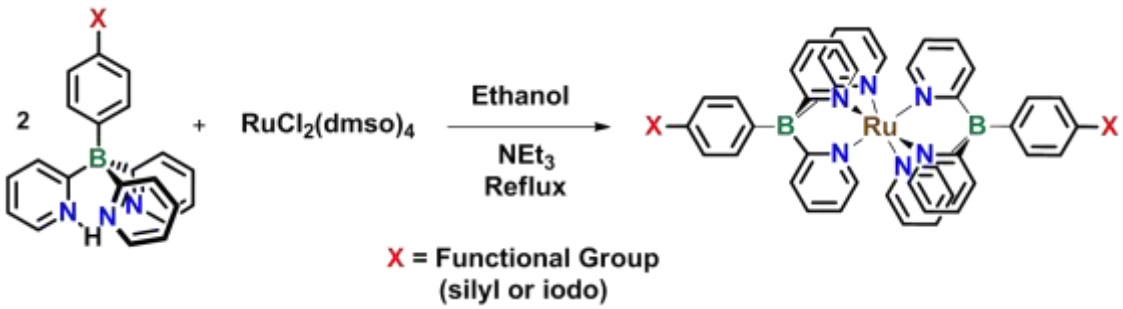

Scheme B3. Synthesis of Ru(Tpyb-X)$_2$ complexes. (X = SiMe$_3$ or I)

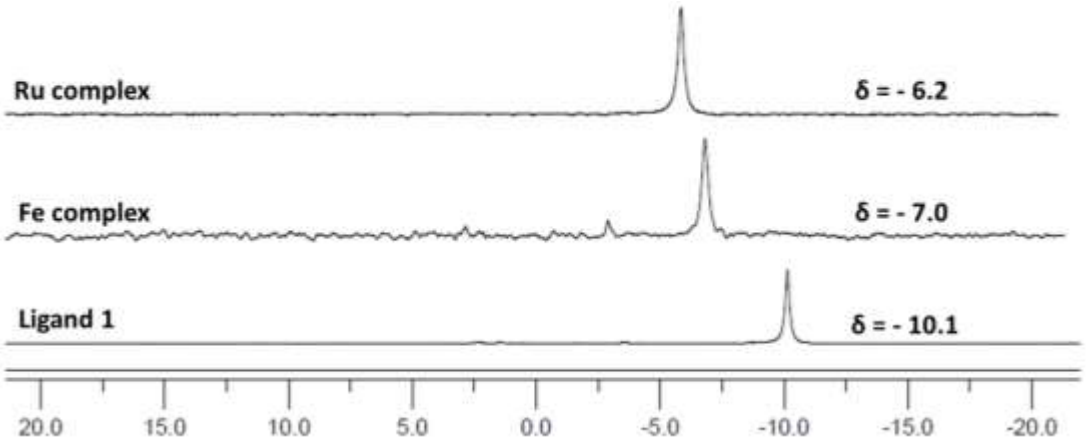

Figure B7. Overlay of ^{11}B NMR spectra of ligand 1 (Tpyb-Si), the Fe(Tpyb-Si)$_2$ and Ru(Tpyb-Si)$_2$ complexes in C_6D_6.

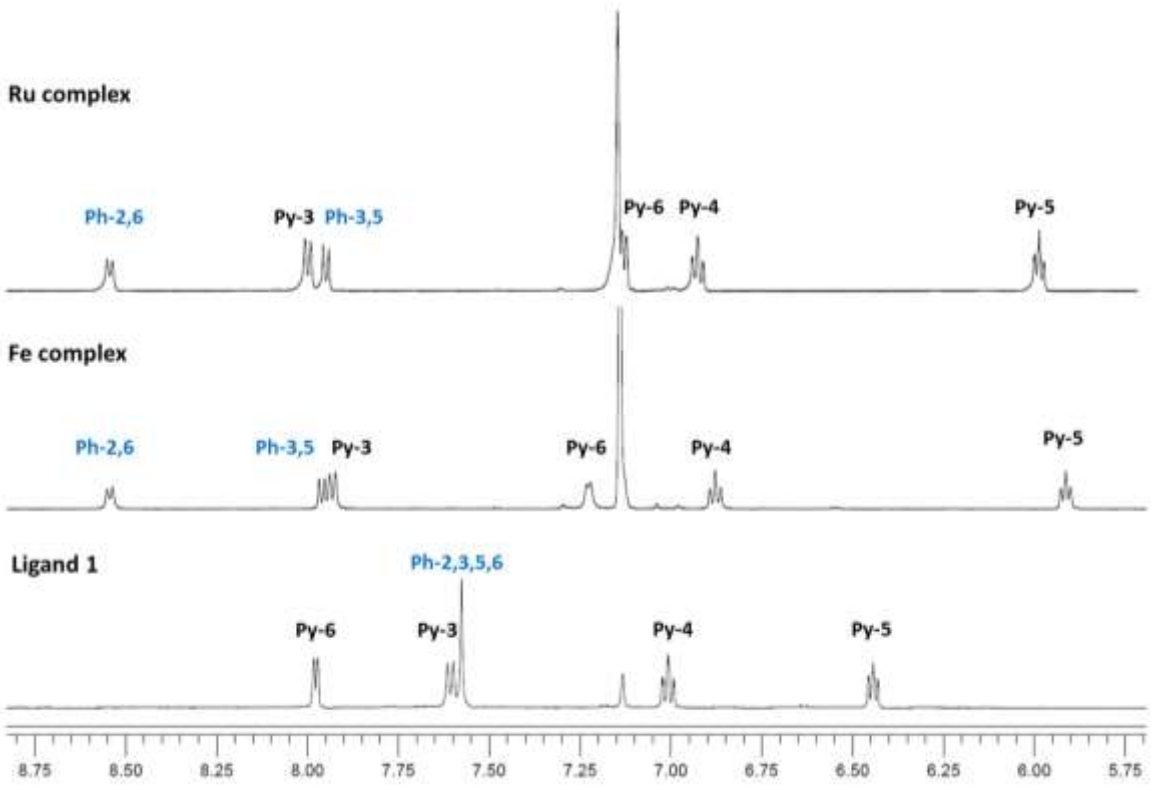

Figure B8. Comparison of the ^{1}H NMR spectra (aromatic region) of ligand 1 (Tpyb-Si), the Fe(Tpyb-Si)$_2$ and Ru(Tpyb-Si)$_2$ complexes in C_6D_6. (Assignments based on comparison to literature data; Chem. Commun. 2012, *48*, 6930-6932.)

B.3.1.1 UV-visible Spectroscopy and Cyclic Voltammetry Data

UV-vis measurements on solutions of Fe(Tpyb-Si)$_2$ and Ru(Tpyb-Si)$_2$ were performed in CH_2Cl_2. Similar maximum absorption wavelengths were observed at ca. 485 and 425-426 (sh) nm for the Fe(II) and at ca. 441-440 and 394 (sh) nm for the Ru(II) complex (Figure B9). In comparison, the corresponding Fe(II) complexes, $[Fe\{(py)_3CH\}_2][NO_3]_2$ (439, 370 nm) and $[Fe\{(py)_3PO\}_2][NO_3]_2$ (465, 385 nm) show similar shapes of the bands in their UV-vis spectra, but at relatively higher energy [4, 9, 17]. In analogy to these literature-

known compounds, the absorption bands of the new Fe(Tpyb-Si)$_2$ and Ru(Tpyb-Si)$_2$ complexes can be assigned to M→L charge transfer (CT). UV-vis measurements for the complexes Fe(Tpyb-I)$_2$ and Ru(Tpyb-I)$_2$ were also carried out and the spectra are nearly identical to those of Fe(Tpyb-Si)$_2$ and Ru(Tpyb-Si)$_2$ (Table B1).

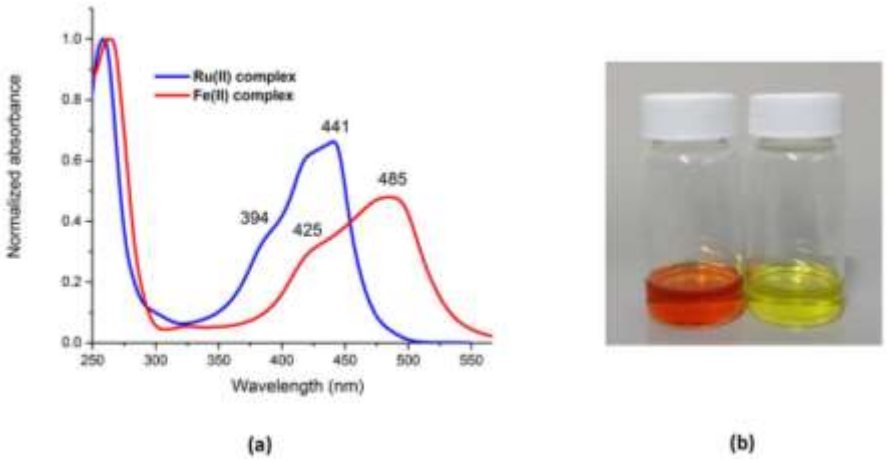

Figure B9. (a) Comparison of UV-vis spectra of Fe(Tpyb-Si)$_2$ and Ru(Tpyb-Si)$_2$ in CH_2Cl_2. (b) Corresponding photographs (left (orange): Fe(Tpyb-Si)$_2$, λ_{max} = 485 nm; right (yellow): Ru(Tpyb-Si)$_2$; λ_{max} = 441 nm).

The redox properties of Fe(Tpyb-Si)$_2$ and Ru(Tpyb-Si)$_2$ were studied by cyclic voltammetry in CH_2Cl_2 using $[Bu_4N]PF_6$ as the electrolyte (Figure B10). The complexes exhibit a redox potential of 180 and 408 mV vs. Ag/AgCl, (–345 and –117 mV vs. $Fc^{+/o}$) respectively. The Fe(Tpyb-Si)$_2$ complex is much more electron-rich than ferrocene and even more easily oxidized than the Tp complex Fe{HB(pz)$_3$}$_3$ (–270 mV vs. $Fc^{+/o}$) [17, 20]. In comparison, the Ru(Tpyb-Si)$_2$ complex is less easily oxidized and thus less electron-

rich. The cyclic voltammetry data of Fe(Tpyb-I)$_2$ and Ru(Tpyb-I)$_2$ were also acquired and they are similar (Table B1), except for that the redox potentials are somewhat larger than for Fe(Tpyb-Si)$_2$ and Ru(Tpyb-Si)$_2$ due to the electron-withdrawing iodo substituents.

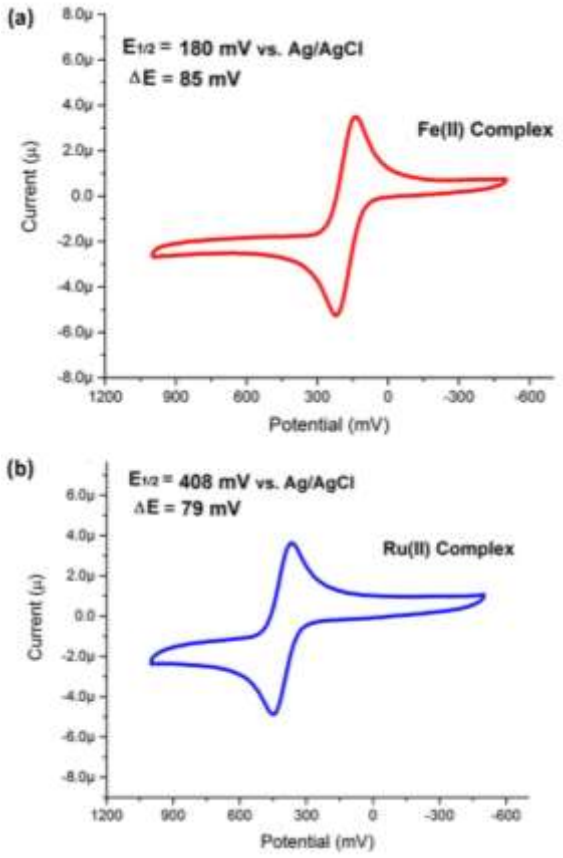

Figure B10. Comparison of cyclic voltammograms of (a) Fe(Tpyb-Si)$_2$ and (b) Ru(Tpyb-Si)$_2$. 1 × 10^{-3}M with 0.1M [Bu_4N]PF_6 in CH_2Cl_2 as the supporting electrolyte (scan rate 100 mV/s; Ag/AgCl was used as reference and set as zero).

Table B1. Summary of the UV-vis absorption and CV Data.

	$\lambda_{max(abs)}$ [nm]	$\lambda_{(sh)\ (abs)}$ [nm]	$E_{1/2}$ [mV]	ΔE [mV]
Fe(Tpyb-Si)$_2$	485	425	180	85
Ru(Tpyb-Si)$_2$	441	394	408	79
Fe(Tpyb-I)$_2$	485	426	247	77
Ru(Tpyb-I)$_2$	440	394	483	82

B.4 Further Functionalization of Metal Complexes

B.4.1 Further Functionalization of Ru(II) Complexes

The Ru(II) complexes were chosen for further functionalization given the better oxidative stability.

B.4.1.1 Introduction of Boryl Groups

We attempted further functionalization of the Ru complexes by introduction of boryl groups (Scheme B4). Our first approach involved reaction of Ru(Tpyb-I)$_2$ with bis(pinacolato)diboron using $PdCl_2$(dppf) as the catalyst and potassium acetate as the base in THF. A yellow/green solid was obtained that was purified by column chromatography on silica gel with a 1:9 mixture of ethyl acetate and hexanes as the eluent. However, MALDI-MS and NMR data revealed only the starting material, indicating that no reaction had occurred.

In an alternative approach, Ru(Tpyb-Si)$_2$ was reacted with excess of boron tribromide in dichloromethane and the mixture then quenched with methoxy(trimethyl)silane. Lastly

reaction with pinacol gave a yellow/green solid that was purified by column chromatography on silica gel with a 1:9 mixture of ethyl acetate and hexanes as the eluent. MALDI-MS analysis indicated successful formation of the product. However, some by-products were also present and further purification is necessary to obtain analytically pure material. Ultimately, we expect that Suzuki-Miyaura coupling reactions with bifunctional iodo species would provide access to new metallo-supramolecular structures (see also Scheme B6).

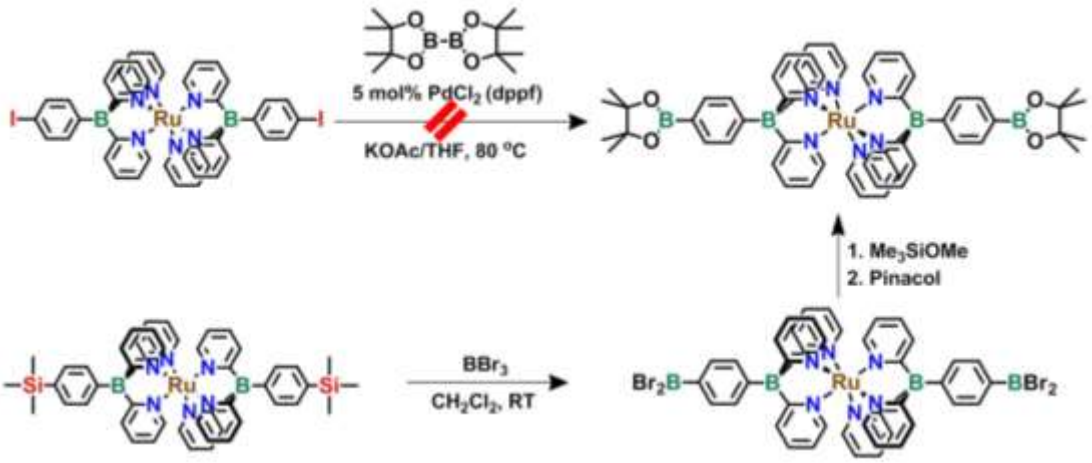

Scheme B4. Attempted further functionalization of metal complexes by introduction of boryl groups.

B.4.1.2 Introduction of Alkynyl Groups

We also attempted further functionalization of the Ru(II) complexes by introduction of alkynyl groups (Scheme B5). In a Sonogashira-Hagihara coupling, the complex $Ru(Tpyb\text{-}I)_2$ was reacted with trimethylsilylacetylene in the presence of piperidine, CuI,

and $Pd(PPh_3)_2Cl_2$ in THF. A yellow/green solid was obtained that was purified by column chromatography on alumina gel with a mixture of hexane and DCM as the eluent. The ^1H NMR shifts of the dialkynyl complexes $Fe(Tpyb\text{-}CCR)_2$ and $Ru(Tpyb\text{-}CCR)_2$ are similar (Figures B11). In the ^{13}C NMR spectra (Figure B12), two sharp peaks at 107 ppm and 92 ppm were assigned to the alkynyl carbons. The characteristic patterns for the pyridyl and phenyl rings were also observed. It is expected that Sonogashira-Hagihara cross coupling reactions with bifunctional iodo species would provide access to metallo-supramolecular polymeric structures (Scheme B6).

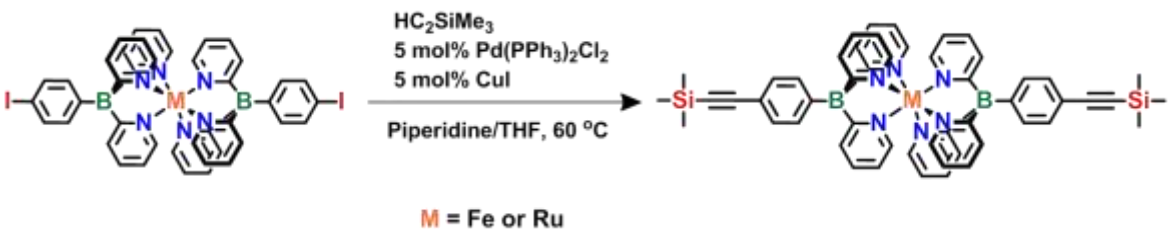

Scheme B5. Further functionalization of metal complexes by introduction of alkynyl groups.

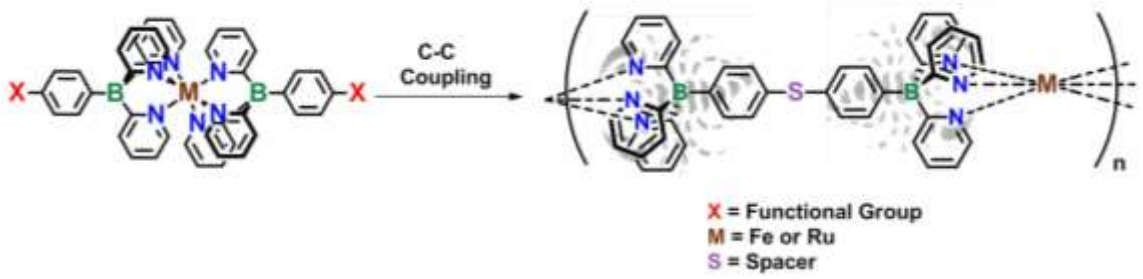

Scheme B6. Proposed synthesis of the metallo-supramolecular polymeric materials by cross-coupling reactions.

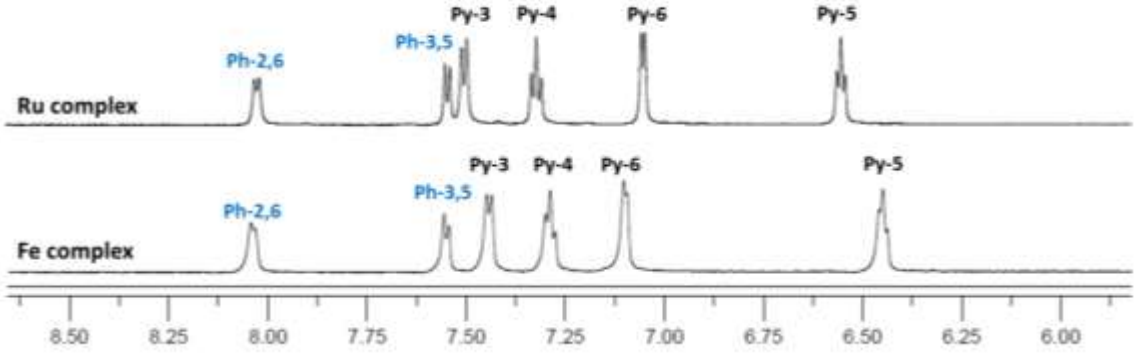

Figure B11. Overlay of ^{1}H NMR spectra (aromatic region) of Fe(Tpyb-CCR)$_2$ and Ru(Tpyb-CCR)$_2$ in THF-d_8. (Assignments based on comparison to literature data; Chem. Commun. 2012, *48*, 6930-6932.)

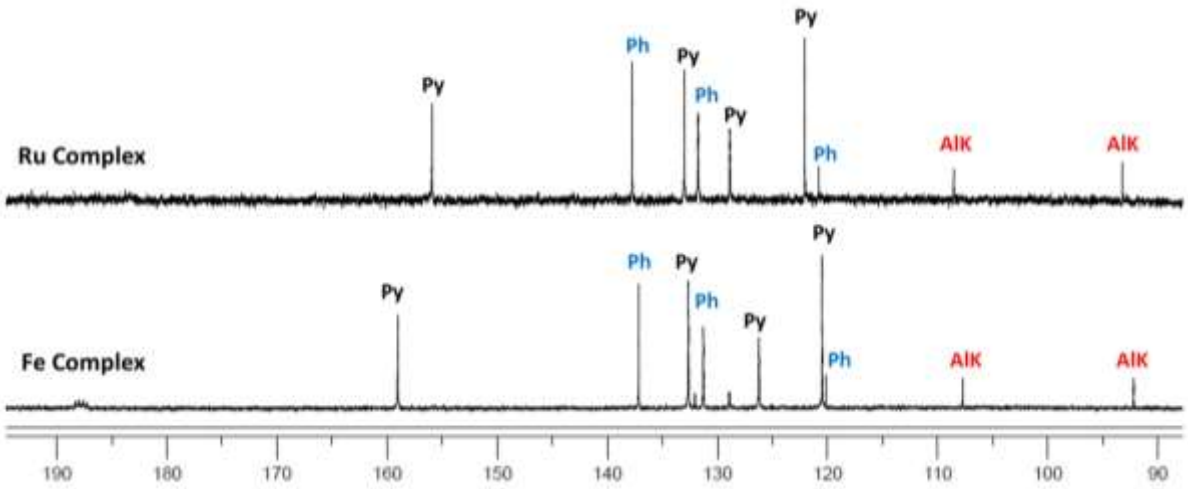

Figure B12. Overlay of ^{13}C NMR spectra (aromatic and alkynyl region) of Fe(Tpyb-CCR)$_2$ and Ru(Tpyb-CCR)$_2$ in THF-d_8. (Assignments based on comparison to literature data; Chem. Commun. 2012, *48*, 6930-6932 and 2D NMR.)

B.5 Development of a Bitopic Ligand

B.5.1 Synthesis and Characterization of the Bifunctional Ligand 3

A multiple-step synthesis for the preparation of ligand 3 ($Tpyb_2$-FL) was developed, in which selective silicon boron exchange is the key step (Scheme B7). 2,7-Bis(dibromoboryl)-9,9-dihexylfluorene was reacted with an excess 2-PyMgCl. The reaction mixture was treated with aqueous $NaHCO_3$ followed by extraction with dichloromethane. The dichloromethane solution was brought to dryness by rotary evaporation and the product was washed with methanol, hexanes, and isopropyl alcohol. A white solid was obtained that was further purified by column chromatography on alumina gel with solvent mixtures of dichloromethane to tetrahydrofuran as eluent.

We also performed preliminary studies on the formation of metallo-supramolecular polymeric materials by metal complexation to $Tpyb_2$-FL (Scheme B8). We attempted the formation of low molecular weight oligomer structures by treatment of $Tpyb_2$-FL with $FeCl_2$ (2:1) and triethylamine in THF. The reaction gave a dark red insoluble part and red soluble part. We also attempted the formation of high molecular weight polymeric material by treatment of $Tpyb_2$-FL with $FeCl_2$ (1:1) and triethylamine in THF. This reaction gave mostly a red orange insoluble material and only very slightly colored solution. A corresponding reaction with $RuCl_2(DMSO)_4$ (2:1) and triethylamine in ethanol gave a larger amount of light green insoluble material and a small amount of soluble component. MALDI-MS analysis of the soluble fractions showed in all cases only the ligand precursor and no metal complexes could be identified. Due to the very low solubility we could not determine the structure of the insoluble material, which is anticipated to contain the desired polymeric materials.

Scheme B7. Synthesis of bifunctional ligand 3 ($Tpyb_2$-FL) (PC = propylene carbonate).

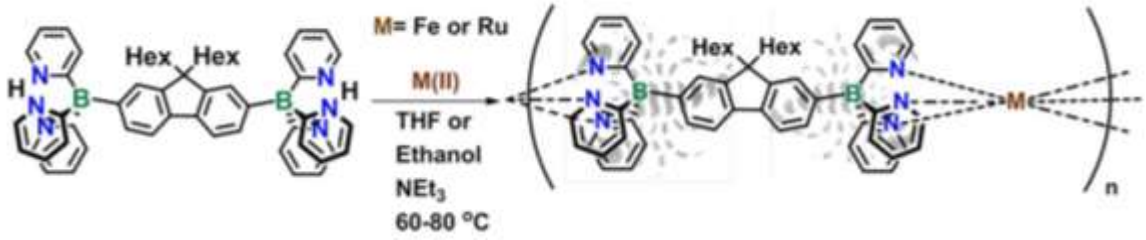

Scheme B8. Attempted synthesis of metallo-supramolecular polymeric materials upon complexation of bifunctional ligand 3 ($Tpyb_2$-FL).

B.5.1.1 NMR Characterization

NMR analysis in $CDCl_3$ was used to identify the bifunctional ligand 3 and the assignments of the protons in the pyridine and fluorene rings are depicted in Figure B13. The ^1H NMR pattern of the pyridine rings is similar to those of the Tpyb-Si and Tpyb-I ligands respectively (Figure B14). The ^1H NMR spectra also feature the expected pattern for the fluorene rings and hexyl groups. A singlet was found at 18.9 ppm that confirms the presence of a nitrogen-bound proton. The ^{11}B NMR spectrum of this compound showed a sharp singlet near -10 ppm, which is in the region expected for tetraarylborates (Figure B15). The ^{13}C NMR spectra exhibited quartets near 184 ppm and 153 ppm which are due to coupling of boron to the boron-bound pyridyl carbon atoms and fluorene carbon atoms, respectively.

Figure B13. Numbering scheme of the pyridine and fluorene rings.

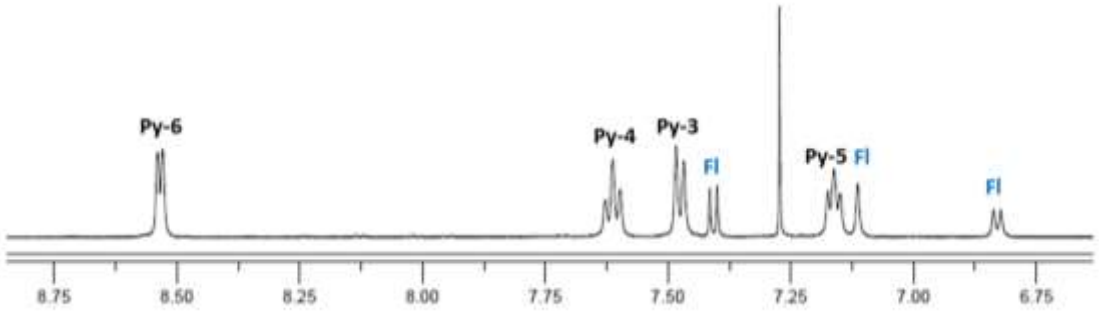

Figure B14. ^{1}H NMR spectrum (aromatic region) of Tpyb$_2$-FL in $CDCl_3$. (Assignments based on comparison to literature data; Chem. Commun. 2012, 48, 6930-6932, Angew. Chem. Int. Ed. 2009, 48, 2313-2316.)

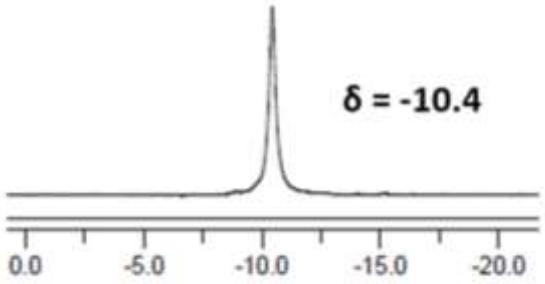

Figure B15. ^{11}B NMR spectrum of Tpyb$_2$-FL in $CDCl_3$.

B.5.1.2 Single Crystal X-ray Diffraction Analysis

The structure of Tpyb$_2$-FL was also determined by single crystal X-ray diffraction analysis (Figure B16). Single crystals for X-ray diffraction analysis were obtained by slow evaporation of a solution in a mixture of hexanes and THF. Based on the single-crystal X-ray data one independent main molecule was found in the unit cell. The

presence of nitrogen-bound protons was confirmed, but the hexyl groups showed some disorder.

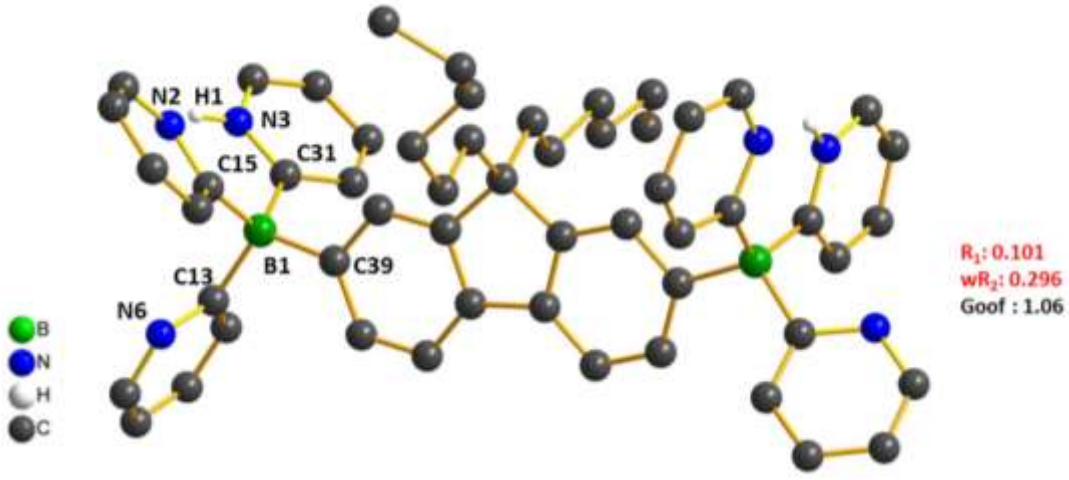

Figure B16. Ball and stick representation of the X-ray structure of $Tpyb_2$-FL. Hydrogen atoms are omitted for clarity except for the acidic protons H1.

B.6 Conclusions and Future Work

We have introduced several examples of functional 2nd generation tris(2-pyridyl)borate (Tpyb) ligands and explored their metal complexes. Scorpionate-type ligands are attracting much attention in the field of supramolecular metallopolymers. We concentrated our attention on the preparation of functional derivatives of the more robust Tpyb ligands as new versatile building blocks to be utilized in supramolecular polymer chemistry. We also anticipate other applications of this new ligand class in the field of materials chemistry and catalysis. The Ru(II) and Fe(II) complexes of the new tris(2-pyridyl)borate ligands have been prepared. UV-vis studies of the metal complexes

revealed the presence of metal-ligand charge transfer (MLCT) bands. Electrochemical studies showed that the Ru(II) complexes are less easily oxidized than the Fe(II) complexes. The complexes also lend themselves to further investigation of their magnetic properties.

We also succeeded in the further functionalization of these metal complexes by introduction of boryl and alkynyl groups. We anticipate the formation of metallo-supramolecular polymeric materials by cross-coupling of these functional metal complexes. In a complimentary approach, we developed the formation of metallo-supramolecular polymeric materials by metal complexation to a bifunctional ligand. However, we have not yet been able to confirm the structure of the products due to their low solubility.

B.7 Experimental Part

B.7.1 Materials and General Methods

Mg, 2-bromopyridine, NEt_3 and anthracene were purchased from Fisher Scientific, $Pd(PPh_3)_2Cl_2$ from Strem Chemical, HC_2SiMe_3 from Oakwood Chemical, dithranol form MP Biochemicals, ethyl alcohol (anhydrous) from Pharmco-AAPER, BBr_3, *n*-BuLi (1.6 M in hexanes), $FeCl_2$ (anhydrous), $RuCl_3 \bullet H_2O$, methoxy(trimethyl)silane, CuI and piperidine from Sigma-Aldrich, fluorene, propylene carbonate and 1,4-diiodobenzene from Alfa Aesar, Me_3SiCl (TMSCl) and pinacol from Acros. All chemicals were used as received without further purification. $RuCl_2(dmso)_4$ [21], 1,4-bis(trimethylsilyl)benzene [19] and 1-iodo-4-trimethylsilylbenzene [22] were synthesized as previously reported. Solvents were purchased from Pharmco and used as received unless noted otherwise. Ether

solvents were distilled from Na/benzophenone prior to use. Hydrocarbon and chlorinated solvents were purified using a solvent purification system (Innovative Technologies; alumina/copper columns for hydrocarbon solvents). Chlorinated solvents were distilled from CaH_2 and degassed via several freeze-pump thaw cycles. 4-Trimethylsilylphenyl dibromoborane [19], 4-iodophenyl dibromoborane [19], 2,7-dibromofluorene [23] [24], 2,7-dibromo-9,9-dihexylfluorene [25] [24], 2,7- bis(trimethylsilyl)-9,9-dihexylfluorene [26], 2,7-bis(dibromoboryl)-9,9-dihexylfluorene [26] and 2-pyridyl magnesium chloride [17] were synthesized by modification of the literature procedures. Reactions and manipulations involving boron halide, iron, and ruthenium species were carried out under an atmosphere of prepurified nitrogen using either Schlenk techniques or an inert-atmosphere glove box (MBraun). All other procedures were carried out under ambient conditions.

The 499.9 or 599.9 MHz ^{1}H, 125.7 or 150.8 MHz ^{13}C, 160.4 or 192.4 MHz ^{11}B NMR, and 99.3 MHz ^{29}Si NMR spectra were recorded on Varian INOVA 500 or 600 MHz spectrometers. The 160.4 or 192.4 MHz ^{11}B NMR spectra were recorded with a boron-free probe using boron-free quartz NMR tubes. The ^{1}H NMR spectra (7.26 ($CDCl_3$), 7.16 (C_6D_6) and 1.72, 3.58 (THF-d_8)) [27] and ^{13}C NMR spectra (77.16 ($CDCl_3$), 128.06 (C_6D_6), 67.21, 25.31 (THF-d_8)) [27] were referenced internally to the solvent peaks. ^{11}B NMR spectra were referenced externally to BF_3•Et_2O ($\delta = 0$) in C_6D_6. ^{29}Si NMR spectra were referenced to $SiMe_4$ ($\delta = 0$). All NMR spectra were obtained at ambient temperature. All chemical shifts are given in ppm. The ^{1}H and ^{13}C NMR assignments are based on the numbering schemes (Figure B2 and B13). Elemental analyses were obtained from Intertek / Quantitative Technolgies Inc., Whitehouse, NJ.

High-resolution MALDI-MS (anthracene or dithranol matrix) data were obtained on an Apex Ultra 7.0 Hybrid FTMS (Bruker Daltonics). The sample was dissolved in chloroform or THF (ca. 1-10mg/mL), mixed with a solution of the matrix (20mg/mL) in a 1:2 (v/v) ratio, and then spotted on the wells of a sample plate.

Single crystal X-ray diffraction intensities were collected on a Smart Apex2 CCD diffractometer at 100 K using Cu Kα (1.54178 Å) radiation. Details of the X-ray diffraction experiments and crystal structure refinements are provided at the end of the Supporting Information.

Cyclic voltammetry (CV) experiments were carried out on a CV-50W analyzer from BAS. The three-electrode system consisted of an Au disk as working electrode, a Pt wire as secondary electrode and a Ag/AgCl reference electrode. The voltammograms were recorded with ca. 10^{-3} to 10^{-4} M solution in CH_2Cl_2 containing $Bu_4N[PF_6]$ (0.1 M) as the supporting electrolyte. The potentials are reported relative to the Ag/AgCl reference. UV-vis absorption data were acquired on an Agilent Technologies Cary Series UV-Vis-NIR spectrophotometer.

B.7.2 Synthetic Procedures

Synthesis of 4-Trimethylsilylphenyl dibromoborane [19]

In a glove box, a solution of 1,4-bis(trimethylsilyl)benzene (2.0g, 9.0mmol) in 10 mL of CH_2Cl_2 was slowly added to a solution of BBr_3 (2.64g, 9.0mmol) in 10 mL of CH_2Cl_2 and then kept stirring overnight. The volatile materials were evaporated under high vacuum for 5 h to give a light green liquid. The product was used without further purification. Yield: 2.8g (97%) ^{1}H NMR (499.976MHz, $CDCl_3$) δ = 8.18 (d, 2H, J = 8.0 Hz, Ph-H3,5),

7.65 (d, 2H, J = 8.0 Hz, Ph-H2,6), 0.32 (s, 9H, $SiMe_3$). ^{11}B NMR (160.419 MHz, $CDCl_3$) $\delta = 57.5$ ($w_{1/2} = 230$ Hz).

Synthesis of Trimethylsilylphenyltris(2-pyridyl)borate Free Acid (Ligand 1, Tpyb-Si)

Under the protection of nitrogen, a solution of trimethylsilylphenyl dibromoborane (15.8g, 49.4mmol) in 70 mL of CH_2Cl_2 was added drop-wise to a solution of 2-PyMgCl (2eq) (52.3g, 99.0mmol) in CH_2Cl_2 (300mL) and the reaction mixture was kept stirring overnight. $Mg_2Cl_2(C_5H_4N)_2(C_4H_8O)_{3.5}$ was used as an empirical formula for the pyridyl Grignard [17] [28] reagent. The mixture was poured into an aqueous $NaHCO_3$ solution (300mL) to give a slurry which was stirred for 3h. The organic and aqueous layers were separated, and the aqueous layer was extracted three times with 150mL of CH_2Cl_2. The combined organic layers were dried over $MgSO_4$, the solvent was removed by rotary evaporation to give a brown solid. The crude product was redissolved in methanol (150mL), filtered, and the methanol-soluble part was concentrated by rotary evaporation to give a dark brown solid. The product was then redissolved in cyclohexane (150mL) with mild heat and filtered. The cyclohexane-soluble part was concentrated by rotary evaporation to give a brown solid. The product was further purified by chromatography on alumina gel with solvent gradients being varied from dichloromethane to tetrahydrofuran. The product was dried under high vacuum at 60℃ for 8h to give a light yellow solid. Yield: 7.5g (38%) ^1H NMR (499.976MHz, $CDCl_3$) $\delta = 18.7$ (br s, 1H, pyridyl N-H), 8.50 (d, $^3J = 5.0$ Hz, 3H, pyridyl-H6), 7.60 (pst, $^3J = 7.5$ Hz, 3H, pyridyl-H4), 7.42 (d, $^3J = 7.5$ Hz, 3H, pyridyl-H3), 7.31 (d, $^3J = 7.5$ Hz, 2H, Ph-H3,5), 7.12 (pst, $^3J = 6.2$ Hz, 3H, pyridyl-H5), 7.05 (br d, $^3J = 6.0$ Hz, 2H, Ph-2,6), 0.21 (s, 9H, $SiMe_3$). ^{13}C NMR (125.732 MHz, $CDCl_3$) $\delta = 183.7$ (q, $J_{C\text{-}B} = 53$ Hz, pyridyl-C2), 156.8 (q, $J_{C\text{-}B} =$

50 Hz, Ph-C1), 143.5 (pyridyl-C6), 136.3 (pyridyl-C4), 135.1 (Ph-C4) 134.0 (Ph-C2,6), 132.3 (Ph-C3,5), 131.7 (pyridyl-C3), 119.8 (pyridyl-C5), -0.8 ($SiMe_3$). ^{11}B NMR (160.411 MHz, $CDCl_3$) $\delta = -10.7$ ($w_{1/2} = 17$ Hz). ^{29}Si NMR (99.331MHz, $CDCl_3$) $\delta = -5.2$. High- resolution MALDI-MS (anthracene, neg. mode): m/z = 394.1891 ($[M-H]^-$, calcd for $^{12}C_{24}{}^{1}H_{26}{}^{11}B_{1}{}^{14}N_{3}{}^{28}Si_{1}$ 394.1910). Single crystals for X-ray diffraction analysis were obtained from a mixture of hexanes and toluene (1:1) at -20 ℃.

The methanol-insoluble fraction from the above work-up procedure was collected as a light yellow solid. The product was washed with cyclohexane, and then dried under high vacuum. The product was identified by NMR spectroscopy to be the corresoponding $Mg(Tpyb\text{-}Si)_2$ complex.

Synthesis of Bis(trimethylsilylphenyltris(2-pyridyl)borate) Magnesium(II) ($Mg(Tpyb\text{-}Si)_2$)

Under the protection of nitrogen, a solution of trimethylsilylphenyl dibromoborane (3.8g, 11.9mmol) in 20 mL of toluene was added drop-wise to a solution of pyridyl Grignard (9.5g, 18.0 mmol) in toluene (250mL) and the reaction mixture was kept stirring overnight. The mixture was poured into an aqueous $NaHCO_3$ solution (300mL) to give a slurry which was stirred for 3h. The organic and aqueous layers were separated, and the aqueous layer was extracted three times with 100mL of CH_2Cl_2. The combined organic layers were dried over $MgSO_4$, and the solvent was removed by rotary evaporation to give a brown solid. The crude product was extracted with methanol (200mL), collected by filtration, washed with cyclohexane, and then dried under high vacuum to give an ivory powder. Yield: 1.01g (21%) ^1H NMR (499.976MHz, $CDCl_3$) $\delta = 8.05$ (br d, J = 7.0

Hz, 4H, Ph-H2,6), 7.70 (d, not resolved, 10H, pyridyl-H3&Ph-H3,5), 7.59 (d, J = 5.0 Hz, 6H, pyridyl-H6), 7.40 (pst, J = 7.0 Hz, 6H, pyridyl-H4), 6.66 (pst, J = 6.2 Hz, 6H, pyridyl-H5), 0.42 (s, 18H, $SiMe_3$). ^{1}H NMR (599.717MHz, THF-d_8) δ = 7.98 (br d, J = 7.2 Hz, 4H, Ph-H2,6), 7.67 (d, J = 7.2 Hz, 6H, pyridyl-H3), 7.64 (d, J = 7.2 Hz, 4H, Ph-H3,5), 7.57 (d, J = 5.4 Hz, 6H, pyridyl-H6), 7.41 (pst, J = 7.8 Hz, 6H, pyridyl-H4), 6.69 (pst, J = 6.3 Hz, 6H, pyridyl-H5), 0.38 (s, 18H, $SiMe_3$).^{13}C NMR (125.732 MHz, $CDCl_3$) δ = 184.4 (q, J_{C-B} = 51 Hz, pyridyl-C2), 154.8 (q, J_{C-B} = 54 Hz, Ph-C1), 148.4 (pyridyl-C6), 136.8 (Ph-C2,6), 135.3 (Ph-C4) 134.9 (Ph-C3,5 or pyridyl-C4), 132.4 (Ph-C3,5 or pyridyl-C4), 129.8 (pyridyl-C3), 118.7 (pyridyl-C5), -0.5 ($SiMe_3$). ^{11}B NMR (160.419 MHz, $CDCl_3$) δ = − 9.0 ($w_{1/2}$ = 16 Hz). ^{29}Si NMR (99.331MHz, $CDCl_3$) δ = − 5.1. High-resolution MALDI-MS (anthracene, pos. mode): m/z = 812.3683 (M^+, calcd for $^{12}C_{48}{}^1H_{50}{}^{11}B_2{}^{24}Mg^{14}N_6{}^{28}Si_2$ 812.3684). Single crystals for X-ray diffraction analysis were obtained by slow evaporation of a solution in cyclohexane.

Synthesis of Bis(trimethylsilylphenyltris(2-pyridyl)borate) Iron(II) (Fe(Tpyb-Si)$_2$)

Under the protection of nitrogen, a 100mL Schlenk flask was charged with anhydrous $FeCl_2$ powder (0.10g, 0.79mmol) and anhydrous tetrahydrofuran (50mL). A solution of trimethylsilylphenyltris(2-pyridyl)borate free acid (0.30g, 0.76 mmol) and triethylamine (1.92 mL, 13.8 mmol) in methanol (10mL) was then added. The reaction mixture was kept stirring for 3h and subsequently filtered to give a red solution. The volatile components were removed on a rotary evaporator to give a red solid, which was purified by column chromatography on silica gel with hexanes and then a 1:9 mixture of tetrahydrofuran and hexanes as the eluent. Solvent evaporation gave the product as a red

solid, which was dried under high vacuum at RT for 3 h. Yield: 45mg (14%) ^{1}H NMR (599.717 MHz, THF-d_8) δ = 8.08 (d, J = 7.2 Hz, 4H, Ph-H2,6), 7.67 (d, J = 7.2 Hz, 4H, Ph-H3,5), 7.55 (d, J = 7.8 Hz, 6H, pyridyl-H3), 7.28 (pst, J = 7.5 Hz, 6H, pyridyl-H4), 7.13 (d, J = 5.4 Hz, 6H, pyridyl-H6), 6.48 (pst, J = 6.3 Hz, 6H, pyridyl-H5), 0.38 (s, 18H, $SiMe_3$). ^{1}H NMR (499.976 MHz, C_6D_6) δ = 8.53 (br d, J = 7.5 Hz, 4H, Ph-H2,6), 7.95 (d, J = 7.0 Hz, 4H, Ph-H3,5), 7.92 (d, J = 7.5 Hz, 6H, pyridyl-H3), 7.23 (d, J = 5.5 Hz, 6H, pyridyl-H6), 6.88 (pst, J = 7.5 Hz, 6H, pyridyl-H4), 5.91 (pst, J = 6.5 Hz, 6H, pyridyl-H5), 0.44 (s, 18H, $SiMe_3$). ^{13}C NMR (125.732 MHz, C_6D_6) δ = 158.8 (pyridyl-C6), 137.0 (Ph-C2,6), 135.8 (Ph-C4), 133.3 (Ph-C3,5 or pyridyl-C4) 132.2 (Ph-C3,5 or pyridyl-C4), 126.3 (pyridyl-C3), 119.9 (pyridyl-C5), -0.5 ($SiMe_3$).^{13}C NMR (150.812 MHz, THF-d_8) δ = 188.4 (q, $J_{C\text{-}B}$ = 50 Hz, pyridyl-C2), 159.0 (pyridyl-C6), 154.3 (q, $J_{C\text{-}B}$ = 57 Hz, Ph-C1), 136.9 (Ph-C2,6), 135.5 (Ph-C4), 132.8 (Ph-C3,5 or pyridyl-C4) 132.4 (Ph-C3,5 or pyridyl-C4), 126.3 (pyridyl-C3), 120.3 (pyridyl-C5), -0.8 ($SiMe_3$). ^{11}B NMR (192.421 MHz, THF-d_8) δ = − 7.4 ($w_{1/2}$ = 18 Hz). High-resolution MALDI-MS (anthracene, pos. mode): m/z = 844.3178 (M^+, calcd for $^{12}C_{48}{}^{1}H_{50}{}^{11}B_2{}^{56}Fe{}^{14}N_6{}^{28}Si_2$ 844.3183).

Synthesis of Bis(trimethylsilylphenyltris(2-pyridyl)borate) Ruthenium(II) ($Ru(Tpyb\text{-}Si)_2$)

Under the protection of nitrogen, to a refluxing solution of $RuCl_2(dmso)_4$ (0.61g, 1.26 mmol) in ethanol (40mL) was added a hot solution of trimethylsilylphenyltris(2-pyridyl)borate free acid (1.00g, 2.53mmol) and triethylamine (1.06mL, 7.59mmol) in ethanol (50 mL) and kept stirring at 110 ℃ for 72 hours. A light brown precipitate formed, which was collected by filtration of the hot suspension and washed with acetone

(2 x 5 mL) and ether (2 x 3 mL). Solvent evaporation gave the product as a yellow/light green solid, which was dried under high vacuum at RT for 5 h. Yield: 0.45g (40%) ^{1}H NMR (599.717 MHz, THF-d_8) δ = 8.07 (br d, J = 6.6 Hz, 4H, Ph-H2,6), 7.66 (d, J = 7.2 Hz, 4H, Ph-H3,5), 7.61 (d, J = 7.2 Hz, 6H, pyridyl-H3), 7.31 (pst, J = 6.6 Hz, 6H, pyridyl-H4), 7.08 (d, J = 5.4 Hz, 6H, pyridyl-H6), 6.55 (pst, J = 5.7 Hz, 6H, pyridyl-H5), 0.38 (s, 18H, $SiMe_3$). ^{1}H NMR (499.976 MHz, C_6D_6) δ = 8.54 (br d, J = 7.0 Hz, 4H, Ph-H2,6), 8.00 (d, J = 7.5 Hz, 6H, pyridyl-H3), 7.94 (d, J = 7.5 Hz, 4H, Ph-H3,5), 7.11 (d, J = 5.5 Hz, 6H, pyridyl-H6), 6.90 (pst, J = 7.2 Hz, 6H, pyridyl-H4), 5.96 (pst, J = 6.0 Hz, 6H, pyridyl-H5), 0.44 (s, 18H, $SiMe_3$). ^{13}C NMR (125.732 MHz, C_6D_6) δ = 183.9 (q, not resolved, pyridyl-C2), δ = 155.5 (pyridyl-C6), 137.1 (Ph-C2,6), 135.8 (Ph-C4), 133.3 (Ph-C3,5 or pyridyl-C4) 132.0 (Ph-C3,5 or pyridyl-C4), 128.5 (pyridyl-C3), 120.8 (pyridyl-C5), -0.5 ($SiMe_3$), Ph-$C1_B$ not observed. ^{11}B NMR (192.421 MHz, THF-d_8) δ = −6.7 ($w_{1/2}$ = 19 Hz). High-resolution MALDI-MS (anthracene, pos. mode): m/z = 890.2879 (M^+, calcd for $^{12}C_{48}{}^{1}H_{50}{}^{11}B_2{}^{101}Ru{}^{14}N_6{}^{28}Si_2$ 890.2885).

Synthesis of 4-Iodophenyl Dibromoborane

In a glove box, a solution of 1-iodo-4-trimethylsilylbenzene (4.00g, 14.5mmol) in 20 mL of CH_2Cl_2 was slowly added to a solution of BBr_3 (1.36mL, 14.3mmol) in 8 mL of CH_2Cl_2 and then kept stirring overnight. The volatile materials were evaporated under high vacuum for 5 h to give a light brown liquid. The product was used without further purification. Yield: 4.5g (84%) ^{1}H NMR (499.976MHz, $CDCl_3$) δ = 7.91 (d, 2H, J = 8.5, Ph-H), 7.87 (d, 2H, J = 8.0 Hz, Ph-H).^{11}B NMR (160.415 MHz, $CDCl_3$) δ = 57.2 ($w_{1/2}$ = 250 Hz).

Synthesis of Iodophenyltris(2-pyridyl)borate Free Acid (Ligand 2, Tpyb-I)

The product was prepared by Patrycja Lupinska and Patrick Shipman. Under the protection of nitrogen, a solution of iodophenyl dibromoborane (4.50g, 12.0mmol) in 50 mL of CH_2Cl_2 was added drop-wise to a solution of pyridyl Grignard (14.4g, 27.3mmol) in CH_2Cl_2 (100mL) and the reaction mixture was kept stirring overnight. The mixture was poured into an aqueous $NaHCO_3$ solution (200mL) to give a light brown slurry which was stirred for 3h. The organic and aqueous layers were separated, and the aqueous layer was extracted three times with 150mL of CH_2Cl_2. The combined organic layers were dried over Na_2SO_4, the solvent was removed by rotary evaporation to give a brown solid. The crude product was redissolved in acetone (150mL) and filtered. The acetone-soluble part was concentrated by rotary evaporation to give a dark brown solid. The product was then redissolved in ethanol (150mL) and filtered. The ethanol-soluble part was concentrated by rotary evaporation to give a dark brown solid. The product was further purified by chromatography on alumina gel with solvent gradients being varied from dichloromethane to methanol. The product was dried under high vacuum at 60℃ for 8h to give a light purple solid. Yield: 1.10g (20%) ^{1}H NMR (499.976MHz, $CDCl_3$) δ = 16.5 (br s, 1H, pyridyl N-H), 8.50 (d, ^{3}J = 5.0 Hz, 3H, pyridyl-H6), 7.59 (pst, ^{3}J = 7.7 Hz, 3H, pyridyl-H4), 7.46 (d, ^{3}J = 8.0 Hz, 2H, Ph-H3,5), 7.37 (d, ^{3}J = 8.0 Hz, 3H, pyridyl-H3), 7.12 (pst, ^{3}J = 6.2 Hz, 3H, pyridyl-H5), 6.84 (br d, ^{3}J = 5.0 Hz, 2H, Ph-H2,6). ^{13}C NMR (125.732 MHz, $CDCl_3$) δ = 183.4 (q, J_{C-B} = 54 Hz, pyridyl-C2), 156.2 (q, not resolved, Ph-C1), 143.7 (pyridyl-C6), 136.9 (pyridyl-C4), 136.3 (Ph-C2,6) 136.2 (Ph-C3,5), 131.5 (pyridyl-C3), 119.9 (pyridyl-C5), 90.6 (Ph-C4). ^{11}B NMR (160.411 MHz, $CDCl_3$) δ = −10.8 ($w_{1/2}$ = 11 Hz). High- resolution MALDI-MS (anthracene, neg. mode):

m/z = 448.0467 ([M−H]$^-$, calcd for $^{12}C_{21}{}^{1}H_{17}{}^{11}B_{1}{}^{14}N_{3}{}^{126}I_{1}$ 448.0480). Patrick Shipman obtained the single crystals of Tpyb-I by slow evaporation of a mixture solution of DCM and hexane and solved the X-ray structure.

Synthesis of Bis(iodophenyltris(2-pyridyl)borate) Iron(II) (Fe(Tpyb-I)$_2$)

The product was prepared by Patrycja Lupinska in analogy to the procedure for bis(trimethylsilylphenyltris(2-pyridyl)borate) iron(II) from $FeCl_2$ (0.061g, 0.48mmol), triethylamine (0.15mL, 1.08mmol) and iodophenyltris(2-pyridyl)borate free acid (0.47g, 1.05mmol) in tetrahydrofuran. The volatile components were removed on a rotary evaporator to give a red solid, which was purified by column chromatography on silica gel with hexanes and then a 1:9 mixture of tetrahydrofuran and hexanes as the eluent. Solvent evaporation gave the product as a red solid, which was dried under high vacuum at RT for 3 h.

Yield: 0.31g (67%) ^{1}H NMR (599.714 MHz, C_6D_6) δ = 7.96 (br d, J = 7.8 Hz, 4H, Ph-H2,6), 7.92 (d, J = 7.8 Hz, 4H, Ph-H3,5), 7.62 (d, J = 7.2 Hz, 6H, pyridyl-H3), 7.13 (d, J = 5.4 Hz, 6H, pyridyl-H6), 6.82 (pst, J = 7.2 Hz, 6H, pyridyl-H4), 5.89 (pst, J = 6.3 Hz, 6H, pyridyl-H5). ^{1}H NMR (599.717 MHz, THF-d_8) δ = 7.85 (br d, J = 7.2 Hz, 4H, Ph-H2,6), 7.81 (d, J = 7.2 Hz, 4H, Ph-H3,5), 7.46 (d, J = 7.8 Hz, 6H, pyridyl-H3), 7.31 (pst, J = 7.2 Hz, 6H, pyridyl-H4), 7.10 (d, J = 4.2 Hz, 6H, pyridyl-H6), 6.48 (pst, J = 6.0 Hz, 6H, pyridyl-H5). ^{13}C NMR (150.812 MHz, C_6D_6) δ = 158.7 (pyridyl-C6), 139.4 (Ph-C3,5), 137.2 (Ph-C2,6), 132.3 (pyridyl-C4) 126.1 (pyridyl-C3), 120.0 (pyridyl-C5), 91.6 (Ph-C4), C_B not observed. ^{13}C NMR (150.812 MHz, THF-d_8) δ = 187.7 (q, J_{C-B} = 50 Hz, pyridyl-C2), δ = 159.0 (pyridyl-C6), 152.9 (q, not resolved, Ph-C1), 139.7 (Ph-C3,5),

137.0 (Ph-C2,6), 132.7 (pyridyl-C4) 126.1 (pyridyl-C3), 120.5 (pyridyl-C5), 91.1 (Ph-C4). ^{11}B NMR (192.421 MHz, C_6D_6) δ = − 7.4 ($w_{1/2}$ = 14 Hz). ^{11}B NMR (192.421 MHz, THF-d_8) δ = − 7.6 ($w_{1/2}$ = 14 Hz). High-resolution MALDI-MS (anthracene, pos. mode): m/z = 952.0320 (M^+, calcd for $^{12}C_{42}{}^{1}H_{32}{}^{11}B_2{}^{56}Fe^{14}N_6{}^{28}I_2$ 952.0322).

Synthesis of Bis(iodophenyltris(2-pyridyl)borate) Ruthenium(II) (Ru(Tpyb-I)$_2$)

The product was prepared in anology to the procedure for bis(trimethylsilylphenyltris(2-pyridyl)borate) ruthenium (II), from $RuCl_2(dmso)_4$ (0.31g, 0.63mmol), triethylamine (0.53mL, 3.80mmol) and iodophenyltris(2-pyridyl)borate free acid (0.57g, 1.27mmol) in ethanol. Yield: 0.45g (72%) ^{1}H NMR (599.717MHz, THF-d_8) δ = 7.86 (br d, J = 6.6 Hz, 4H, Ph-H2,6), 7.81 (d, J = 7.8 Hz, 4H, Ph-H3,5), 7.53 (d, J = 7.8 Hz, 6H, pyridyl-H3), 7.34 (pst, J = 7.2 Hz, 6H, pyridyl-H4), 7.06 (d, J = 5.4 Hz, 6H, pyridyl-H6), 6.56 (pst, J = 6.3 Hz, 6H, pyridyl-H5). ^{1}H NMR (499.976 MHz, C_6D_6) δ = 8.01 (br d, J = 7.0 Hz, 4H, Ph-H2,6), 8.00 (d, J = 8.5 Hz, 4H, Ph-H3,5), 7.73 (d, J = 8.0 Hz, 6H, pyridyl-H3), 7.06 (d, J = 5.0 Hz, 6H, pyridyl-H6), 6.88 (pst, J = 6.7 Hz, 6H, pyridyl-H4), 5.97 (pst, J = 6.2 Hz, 6H, pyridyl-H5). ^{13}C NMR (150.812 MHz, THF-d_8) δ = 183.3 (q, $J_{C\text{-}B}$ = 53 Hz, pyridyl-C2), 155.7 (pyridyl-C6), 153.6 (q, $J_{C\text{-}B}$ = 56 Hz, Ph-C1), 139.8 (Ph-C3,5), 136.9 (Ph-C2,6), 132.6 (pyridyl-C4), 128.3 (pyridyl-C3), 121.5 (pyridyl-C5), 91.1 (Ph-C4). ^{11}B NMR (192.421 MHz, THF-d_8) δ = − 6.8 ($w_{1/2}$ = 12 Hz). High-resolution MALDI-MS (anthracene, pos. mode): m/z = 997.9996 (M^+, calcd for $^{12}C_{42}{}^{1}H_{32}{}^{11}B_2{}^{101}Ru\ ^{14}N_6{}^{28}I_2$ 998.0025).

Synthesis of Bis(trimethylsilylethynylphenyltris(2-pyridyl)borate) Iron(II) ($Fe(Tpyb\text{-}CCR)_2$)

The product was prepared by Patrycja Lupinska. A Schlenk flask was charged with the bis(iodophenyltris(2-pyridyl)borate) iron(II) complex (0.30g, 0.32mmol), trimethylsilylacetylene (0.060g, 0.61mmol) and piperidine (6.67mL, 1:3 v/v) in tetrahydrofuran (20mL). The reaction vessel and the reactants were then subjected to three freeze/pump/thaw cycles. The reaction mixture was once again frozen, the vessel back-filled with N_2, and then CuI (3.0mg, 5mol-%) and $Pd(PPh_3)_2Cl_2$ (10mg, 5mol-%) were added under a N_2 atmosphere. The flask was then placed in a 60 ℃ oil bath for 2 days. The mixture was poured into an aqueous $NaHCO_3$ solution (50mL) and stirred for 10mins. The organic and aqueous layers were separated, and the aqueous layer was extracted three times with 50mL of CH_2Cl_2. The combined organic layers were dried over $MgSO_4$ and the solvent was removed by rotary evaporation to give a red solid. The product was purified by chromatography on alumina gel with solvent gradients being varied from hexanes to dichloromethane. The product was dried under high vacuum at 50 ℃ for 5h to give a red solid. Yield: 60mg (22%) ^{1}H NMR (599.714MHz, THF-d_8) δ = 8.05 (br d, J = 7.2 Hz, 4H, Ph-H2,6), 7.57 (d, J = 7.2 Hz, 4H, Ph-H3,5), 7.46 (d, J = 7.8Hz, 6H, pyridyl-H3), 7.31 (pst, J = 7.2 Hz, 6H, pyridyl-H4), 7.12 (d, J = 4.8 Hz, 6H, pyridyl-H6), 6.48 (pst, J = 6.0Hz, 6H, pyridyl-H5), 0.28 (s, 18H, $SiMe_3$). ^{13}C NMR (150.812 MHz, THF-d_8) δ = 187.8 (q, $J_{C\text{-}B}$ = 49 Hz, pyridyl-C2), 159.0 (pyridyl-C6), 137.2 (Ph-C2,6), 132.6 (pyridyl-C4) 131.3 (Ph-C3,5), 126.2 (pyridyl-C3), 120.5 (pyridyl-C5), 120.2 (Ph-C4), 107.7 (alkynyl-C1), 92.2 (alkynyl-C2), 0.08 ($SiMe_3$), Ph-$C1_B$ not observed. ^{11}B NMR (192.421 MHz) δ = − 7.5 ($w_{1/2}$ = 17 Hz). High-resolution MALDI-

MS (anthracene, pos. mode): m/z = 892.3171 (M^+, calcd for $^{12}C_{52}{}^{1}H_{50}{}^{11}B_2{}^{56}Fe\,{}^{14}N_6{}^{28}Si_2$ 892.3184).

Synthesis of Bis(trimethylsilylethynylphenyltris(2-pyridyl)borate) Ruthenium(II) (Ru(Tpyb-CCR)$_2$)

The product was prepared in analogy to the procedure for Fe(Tpyb-CCR)$_2$ from bis(iodophenyltris(2-pyridyl)borate) ruthenium(II) (0.20g, 0.20mmol), trimethylsilylacetylene (41mg, 0.42mmol) and piperidine (6.67mL, 1:3 v/v) in tetrahydrofuran (20mL). The product was dried under high vacuum at 50 °C for 5h to give a yellow-green solid. Yield: 90mg (48%) ^{1}H NMR (599.714 MHz, THF-d_8) δ = 8.05 (d, J = 7.2 Hz, 4H, Ph-H2,6), 7.57 (d, J = 7.8 Hz, 4H, Ph-H3,5), 7.52 (d, J = 7.8 Hz, 6H, pyridyl-H3), 7.34 (pst, J = 7.5 Hz, 6H, pyridyl-H4), 7.07 (d, J = 5.4 Hz, 6H, pyridyl-H6), 6.56 (pst, J = 6.3 Hz, 6H, pyridyl-H5), 0.29 (s, 18H, $SiMe_3$). ^{1}H NMR (599.714 MHz, C_6D_6) δ = 8.27 (br d, J = 7.2 Hz, 4H, Ph-H2,6), 7.93 (d, J = 7.8 Hz, 4H, Ph-H3,5), 7.71 (d, J = 7.8 Hz, 6H, pyridyl-H3), 7.04 (d, J = 5.4 Hz, 6H, pyridyl-H6), 6.83 (pst, J = 7.2 Hz, 6H, pyridyl-H4), 5.95 (pst, J = 6.6 Hz, 6H, pyridyl-H5), 0.29 (s, 18H, $SiMe_3$). ^{13}C NMR (150.812 MHz, THF-d_8) δ = 183.4 (q, $J_{C\text{-}B}$ = 48 Hz, pyridyl-C2), 155.7 (pyridyl-C6), 137.3 (Ph-C2,6), 132.5 (pyridyl-C4), 131.2 (Ph-C3,5), 128.3 (pyridyl-C3), 121.4 (pyridyl-C5), 120.1 (Ph-C4), 107.7 (alkynyl-C1), 92.2 (alkynyl-C2), 0.08 ($SiMe_3$), Ph-$C1_B$ not observed. ^{11}B NMR (192.421 MHz, THF-d_8) δ = − 6.8 ($w_{1/2}$ = 17 Hz). High-resolution MALDI-MS (dithranol, pos. mode): m/z = 938.2847 (M^+, calcd for $^{12}C_{52}{}^{1}H_{50}{}^{11}B_2{}^{101}Ru\,{}^{14}N_6{}^{28}Si_2$ 938.2887).

Synthesis of Bis((pinacolatoboryl)phenyltris(2-pyridyl)borate) Ruthenium(II) ($Ru(Tpyb\text{-}Bpin)_2$)

A Schlenk flask was charged with $Ru(Tpyb\text{-}I)_2$ complex (0.10g, 0.10mmol), bis(pinacolato)diboron (0.050g, 0.20mmol) and potassium acetate (0.060g, 0.60mmol) in tetrahydrofuran (35mL) under a N_2 atmosphere. The reaction vessel and the reactants were then subjected to two freeze/pump/thaw cycles. The reaction mixture was once again frozen, the vessel back-filled with N_2, and then $PdCl_2(dppf)$ (4mg, 5mol-%) was added under a N_2 atmosphere. The flask was then placed in a 80℃ oil bath for 3 days. The mixture was poured into an aqueous $NaHCO_3$ solution (50mL) and stirred for 10mins. The organic and aqueous layers were separated, and the aqueous layer was extracted three times with 50mL of benzene. The combined organic layers were dried over $MgSO_4$ and the solvent was removed by rotary evaporation to give a brown solid. The product was purified by column chromatography on silica gel (EtOAc/hexane, 1:9) to give a yellow-green solid that was dried under high vacuum at 50 ℃ for 5h. NMR and MALDI-MS analysis of the crude product and isolated fraction showed only the presence of the iodo-functionalized starting material.

Alternative Procedure: In a glove box, to a solution of $Ru(Tpyb\text{-}Si)_2$ complex (0.20g, 0.22mmol) in 40mL of CH_2Cl_2 was slowly added a solution of BBr_3 (0.060mL, 0.63mmol) in 10mL of CH_2Cl_2 and the mixture was kept stirring overnight. Methoxy(trimethyl)silane (0.93mL, 6.7mmol) was then added neat and the reaction was kept stirring overnight. Pinacol (0.79g, 6.7mmol) and a small amount of molecular sieves were added and the mixture was kept stirring at room temperature under a N2 atmosphere overnight. The crude product was filtered and the soluble part was then concentrated by rotary

evaporation to give a dark brown/green solid. The product was purified by column chromatography on silica gel (EtOAc/Hexane, 2:98), to afford a yellowish solid. MALDI-MS, ^{1}H and ^{11}B NMR analysis of the crude material revealed the desired product, along with some by-products. Further purification of the product is in progress. ^{11}B NMR (192.412 MHz, THF-d_8) $\delta = -6.6$ ($w_{1/2} = 18$ Hz), 0.15 ($w_{1/2} = 1010$ Hz), 32.0 ($w_{1/2} = 1200$ Hz). High-resolution MALDI-MS (dithranol, pos. mode): m/z = 997.3790 (M^+, calcd for $^{12}C_{54}{}^{1}H_{56}{}^{11}B_4{}^{14}N_6{}^{16}O_4{}^{101}Ru$ 997.3823), 874.1711 (ion could not be assigned).

Synthesis of 2,7-Dibromofluorene [23] [24]

A mixture containing fluorene (12.5g, 75mmol), N-bromosuccinimide (27.4g, 153mmol) and propylene carbonate (90mL) was stirred at reflux for 3 h. The mixture was poured into 300mL of methanol and cooled to -20℃ for 1 day. The resulting light brown precipitate was collected by filtration, taken up in hot ethanol, followed by crystallization for 1 day at -20℃. After filtration, the crystalline solid residue was washed with acetic acid with mild heat and filtered to give a light yellow solid. Yield: 16.4g (68%). ^{1}H NMR (499.976 MHz, $CDCl_3$) δ = 7.66 (s, 2H, Fl), 7.59 (d, J = 8.0 Hz, 2H, Fl), 7.51 (dd, J = 8.0 Hz, 2H, Fl), 3.85 (s, 2H, Fl).

Synthesis of 2,7-Dibromo-9,9-dihexylfluorene [25] [24]

Under the protection of nitrogen, 2,7-dibromofluorene (1.4g, 4.3mmol) and 1-bromohexane (2.3mL, 16.4mmol) were dissolved in 11mL of tetrahydrofuran and the mixture stirred for 15 mins. A solution of potassium tert-butoxide (1.10g, 10.0mmol) in 15mL of tetrahydrofuran was slowly added and the reaction mixture was kept stirring for

3h at 0℃. The reaction mixture was allowed to warm to RT and kept stirring overnight under air. The mixture was then poured into an aqueous ammonium chloride solution (150mL). The organic and aqueous layers were separated, and the aqueous layer was extracted three times with 100mL of hexanes. The combined organic layers were dried over $MgSO_4$, and the solvent was removed by rotary evaporation to give a yellow solid. After recrystallization from hot ethanol and subsequent filtration, the product was obtained as a light yellow solid. Yield: 1.6g (77%) ^{1}H NMR (499.976 MHz, $CDCl_3$) δ = 7.53 (d, J = 8.5 Hz, 2H, Fl), 7.46 (s/d, J = 7.5 Hz, 4H, Fl), 1.93 (m, 4H, Hex), 1.16-1.06 (m, 12H, Hex), 0.80 (t, J = 7.2 Hz, 6H, Hex), 0.61 (m, 4H, Hex).

Synthesis of 2,7-Bis(trimethylsilyl)-9,9-dihexylfluorene [26]

Under the protection of nitrogen, 2,7-dibromo-9,9-dihexylfluorene (8.46g, 17.2mmol) and TMEDA (6.2mL, 41.3mmol) were dissolved in diethyl ether (180mL) and cooled to -78℃. A solution of n-BuLi in hexanes (25.8mL, 1.6M, 41.3mmol) was then slowly added. After complete addition the reaction mixture was stirred for 1.5 h at -78℃. The resulting yellow suspension was allowed to slowly warm up to RT and kept stirring for 1.5 h. After cooling back to -78℃ again, the reaction was quenched by addition of neat Me_3SiCl (5.17mL, 40.7mmol) by syringe, and the mixture was stirred for an additional 30mins and kept stirring at RT overnight. The reaction mixture was poured into an aqueous $NaHCO_3$ solution (150mL). The organic and aqueous layers were separated, and the aqueous layer was extracted three times with 100mL of diethyl ether. The combined organic layers were dried over $MgSO_4$, and the solvent was removed by rotary evaporation to give a light yellow oil. The residue was subjected to sublimation under

high vacuum to give a light yellow solid. Yield: 7.5g (91%) ^{1}H NMR (499.976 MHz, $CDCl_3$) δ = 7.71 (d, J = 7.5 Hz, 2H, Fl), 7.50 (s/d, J = 8.0 Hz, 4H, Fl), 1.98 (m, 4H, Hex), 1.14-1.08 (m, 12H, Hex), 0.79 (t, J = 7.0 Hz, 6H, Hex), 0.70 (m, 4H, Hex), 0.34 (s, 18H, $SiMe_3$).

Synthesis of 2,7-Bis(dibromoboryl)-9,9-dihexylfluorene [26]

Under the protection of nitrogen, 2,7-bis(trimethylsilyl)-9,9-dihexylfluorene (9.50g, 19.8mmol) was dissolved in CH_2Cl_2 (90mL) and cooled to -35℃, followed by slowly adding a solution of BBr_3 (4.95mL, 52.1mmol) in 15mL of CH_2Cl_2. The reaction mixture was allowed to warm up to RT and kept stirring for 2 h. The volatile materials were evaporated under high vacuum to give a light green solid. In a glove box, the resulting mixture was taken up in hot hexanes, filtered through a pipet with a kim wipe plug and then stored at -35℃. Light green crystals were obtained, isolated by decantation and dried under high vacuum. Yield: 10.4g (78%) ^{1}H NMR (499.976 MHz, $CDCl_3$) δ = 8.30 (d, J = 8.0 Hz, 2H, Fl), 8.23 (s, 2H, Fl), 7.90 (d, J = 7.5 Hz, 2H, Fl), 2.10 (m, 4H, Hex), 1.11-1.03 (m, 12H, Hex), 0.77 (t, J = 7.0 Hz, 6H, Hex), 0.62 (m, 4H, Hex). ^{11}B NMR (160.419 MHz, $CDCl_3$) δ = 56.9 ($w_{1/2}$ = 750 Hz).

Synthesis of 2,7-Bis(tris(2-pyridyl)borate)-9,9-dihexylfluorene Free Acid (Ligand 3, $Tpyb_2$-FL)

Under the protection of nitrogen, a solution of 2,7-bis(dibromoboryl)-9,9-dihexylfluorene (10.3g, 15.3mmol) in 110mL of CH_2Cl_2 was added drop-wise to a solution of pyridyl Grignard 2-PyMgCl (3eq) (48.7g, 92.2mmol) in CH_2Cl_2 (350mL) and kept stirring

overnight. $Mg_2Cl_2(C_5H_4N)_2(C_4H_8O)_{3.5}$ was used as an empirical formula for the pyridyl Grignard [17] [28] reagent. The mixture was then poured into an aqueous $NaHCO_3$ solution (300mL) to give a slurry which was stirred for 3h. The organic and aqueous layers were separated, and the aqueous layer was extracted three times with 100mL of CH_2Cl_2. The combined organic layers were dried over $MgSO_4$, then the solvent was removed by rotary evaporation to give a yellow brown solid. The crude product was redissolved in methanol (100mL) and filtered. The methanol-soluble part was concentrated by rotary evaporation to give a dark brown solid. This fraction was extracted with hexanes (150mL) and then redissolved in isopropyl alcohol (100mL) with mild heat. The resulting dark brown solution was cooled to -20℃ for 1 day and filtered cold, and the solvent was then removed under vacuum to give a brown solid. Lastly, the product was further purified by chromatography on alumina gel with solvent gradients being varied from dichloromethane to tetrahydrofuran. The product was dried under high vacuum at 60℃ for 8h to give a white solid. Yield: 1.1g (9%) ^{1}H NMR (499.976MHz, $CDCl_3$) δ = 18.9 (br s, 2H, pyridyl N-H), 8.53 (d, ^{3}J = 5.0 Hz, 6H, pyridyl-H6), 7.61 (pst, ^{3}J = 7.7 Hz, 6H, pyridyl-H4), 7.48 (d, ^{3}J = 8.5 Hz, 6H, pyridyl-H3), 7.41 (d, J = 7.5 Hz, 2H, Fl), 7.16 (pst, J = 6.2 Hz, 6H, pyridyl-H5), 7.11 (s, 2H, Fl) 6.83 (d, J = 7.5 Hz, 2H, Fl), 1.66 (m, 4H, Hex), 1.10 (m, 4H, Hex), 1.01-0.93 (m, 8H, Hex), 0.80 (t, J = 7.2 Hz, 6H, Hex), 0.65-0.59 (m, 4H, Hex). ^{13}C NMR (125.732 MHz, $CDCl_3$) δ = 184.2 (q, not resolved, pyridyl-C2), 153.7 (q, not resolved, Fl-C2,7), 149.6 (Fl-C), 143.4 (pyridyl-C6), 138.7 (Fl-C), 136.4 (pyridyl-C4), 132.5 (Fl-C), 131.8 (pyridyl-C3), 129.4 (Fl-C), 119.8 (pyridyl-C5), 118.0 (Fl-C), 54.2 (Fl-C9), 40.3 (Hex), 31.7 (Hex), 29.9 (Hex), 24.0 (Hex), 22.7 (Hex), 14.3 (Hex). ^{11}B NMR (160.419 MHz, $CDCl_3$) δ = −10.4 Hz ($w_{1/2}$ = 30 Hz). High-

resolution MALDI-MS (anthracene, neg. mode): m/z = 823.4868 ($[M-H]^-$, calcd for $^{12}C_{55}{}^{1}H_{58}{}^{11}B_2{}^{14}N_6$ 823.4842). Single crystals for X-ray diffraction analysis were obtained by slow evaporation of a solution in toluene.

Attempted Synthesis of a Supramolecular Polymer from 2,7-Bis(tris(2-pyridyl)borate)-9,9-dihexylfluorene Free Acid ($Tpyb_2$-FL) and Iron(II) Chloride

(1) Attempted Formation of High Molecular Weight Polymer ($Tpyb_2$-FL to $FeCl_2$ ratio = 1:1): A Schlenk flask was charged with 2,7-bis(tris(2-pyridyl)borate)-9,9-dihexylfluorene free acid (0.050g, 0.061mmol) and a solution of triethylamine (0.085mL, 0.61mmol) in 18mL of tetrahydrofuran. A solution of $FeCl_2$ (8.4mg, 0.067mmol) in 17mL of tetrahydrofuran was added drop-wise. Then the flask was placed in a 77 ℃ oil bath under a N_2 atmosphere for 2 days. A red orange insoluble fraction (50mg) was isolated by filtration. The filtrate contained very little product and MALDI-MS analysis showed only the ligand precursor. The product (insoluble part) has a low solubility in common organic solvents and the structure could therefore not be confirmed.

(2) Attempted Formation of Low Molecular Weight Oligomers ($Tpyb_2$-FL to $FeCl_2$ ratio = 2:1): A Schlenk flask was charged with 2,7-bis(tris(2-pyridyl)borate)-9,9-dihexylfluorene free acid (0.050g, 0.061mmol) and a solution of triethylamine (0.085mL, 0.61mmol) in 18mL of tetrahydrofuran. A solution of $FeCl_2$ (4.0mg, 0.032mmol) in 17mL of tetrahydrofuran was added drop-wise. Then the flask was placed in a 77 ℃ oil bath under a N_2 atmosphere for 2 days. A dark red insoluble fraction (15mg) and a red solution were obtained. The crude product was filtered and a dark red solid isolated.

Although the amount soluble material was larger than in the 1:1 experiment, MALDI-MS analysis showed only the ligand precursor and no metal complexes could be identified.

Attempted Synthesis of a Supramolecular Polymer from 2,7-Bis(tris(2-pyridyl)borate)-9,9-dihexylfluorene Free Acid $Tpyb_2$-FL and Ruthenium(II) Chloride

Attempted Formation of Low Molecular Weight Oligomers ($Tpyb_2$-FL to $RuCl_2(dmso)_4$ ratio = 2:1): Under the protection of nitrogen, to a refluxing solution of $RuCl_2(dmso)_4$ (0.015g, 0.031mmol) in ethanol (20mL) was added a hot solution of 2,7-bis(tris(2-pyridyl)borate)-9,9-dihexylfluorene free acid (0.050g, 0.061mmol) and triethylamine (0.085mL, 0.61mmol) in ethanol (20mL) and the mixture was then kept stirring at 90℃ under a N_2 atmosphere for 3 days. A light green precipitate formed, which was collected by filtration of the hot suspension and washed with acetone (2 x 5 mL) and ether (2 x 3 mL). The yield of the crude product was 10mg. The filtrate contained very little product and MALDI-MS analysis showed only the ligand precursor. The product (insoluble part) has a low solubility in common organic solvents and the structure could therefore not be confirmed.

B.8 References

[1] G. R. Whittell, I. Manners, *Advanced Materials* 2007, *19*, 3439-3468.
[2] C.-L. Ho, W.-Y. Wong, *Coordination Chemistry Reviews* 2011, *255*, 2469-2502.
[3] J. B. Beck, J. M. Ineman, S. J. Rowan, *Macromolecules* 2005, *38*, 5060-5068.
[4] M. Burnworth, D. Knapton, S. Rowan, C. Weder, *J Inorg Organomet Polym* 2007, *17*, 91-103.
[5] D. Knapton, S. J. Rowan, C. Weder, *Macromolecules* 2005, *39*, 651-657.
[6] J. D. Fox, S. J. Rowan, *Macromolecules* 2009, *42*, 6823-6835.
[7] D. Knapton, P. K. Iyer, S. J. Rowan, C. Weder, *Macromolecules* 2006, *39*, 4069-4075.
[8] H. Hofmeier, U. S. Schubert, *Chemical Society Reviews* 2004, *33*, 373-399.
[9] C. A. Fustin, P. Guillet, U. S. Schubert, J. F. Gohy, *Advanced Materials* 2007, *19*, 1665-1673.
[10] A. Wild, A. Winter, F. Schlutter, U. S. Schubert, *Chemical Society Reviews* 2011, *40*, 1459-1511.
[11] S. Trofimenko, *Journal of the American Chemical Society* 1966, *88*, 1842-1844.
[12] C. Cui, P. R. Shipman, R. A. Lalancette, F. Jäkle, *Inorganic Chemistry* 2013, *52*, 9440-9448.
[13] S. Trofimenko, *Journal of the American Chemical Society* 1967, *89*, 6288-6294.
[14] D. L. Reger, J. R. Gardinier, W. R. Gemmill, M. D. Smith, A. M. Shahin, G. J. Long, L. Rebbouh, F. Grandjean, *Journal of the American Chemical Society* 2005, *127*, 2303-2316.
[15] G. L. Hillhouse, B. L. Haymore, *Journal of the American Chemical Society* 1982, *104*, 1537-1548.
[16] F. Fabrizi de Biani, F. Jäkle, M. Spiegler, M. Wagner, P. Zanello, *Inorganic Chemistry* 1997, *36*, 2103-2111.
[17] C. Cui, R. A. Lalancette, F. Jakle, *Chemical Communications* 2012, *48*, 6930-6932.
[18] P. O. Shipman, C. Cui, P. Lupinska, R. A. Lalancette, J. B. Sheridan, F. Jäkle, *ACS Macro Letters* 2013, *2*, 1056-1060.
[19] Y. Qin, I. Kiburu, S. Shah, F. Jäkle, *Organic Letters* 2006, *8*, 5227-5230.
[20] D. C. L. De Alwis, F. A. Schultz, *Inorganic Chemistry* 2003, *42*, 3616-3622.
[21] I. P. Evans, A. Spencer, G. Wilkinson, *Journal of the Chemical Society, Dalton Transactions* 1973, 204-209.
[22] D. L. Reger, J. R. Gardinier, M. D. Smith, A. M. Shahin, G. J. Long, L. Rebbouh, F. Grandjean, *Inorganic Chemistry* 2005, *44*, 1852-1866.
[23] W. Y. Huang, S. Y. Huang, *Macromolecules* 2010, *43*, 10355-10365.
[24] M. Ranger, D. Rondeau, M. Leclerc, *Macromolecules* 1997, *30*, 7686-7691.
[25] M.-Y. Yuen, S. C. F. Kui, K.-H. Low, C.-C. Kwok, S. S.-Y. Chui, C.-W. Ma, N. Zhu, C.-M. Che, *Chemistry – A European Journal* 2010, *16*, 14131-14141.
[26] H. Li, F. Jäkle, *Angewandte Chemie International Edition* 2009, *48*, 2313-2316.
[27] G. R. Fulmer, A. J. M. Miller, N. H. Sherden, H. E. Gottlieb, A. Nudelman, B. M. Stoltz, J. E. Bercaw, K. I. Goldberg, *Organometallics* 2010, *29*, 2176-2179.

[28] A. V. Churakov, D. P. Krut'ko, M. V. Borzov, R. S. Kirsanov, S. A. Belov, J. A. K. Howard, *Acta Crystallographica Section E* 2006, *62*, m1094-m1096.

Appendix

Appendix A.1 The following tables are supplementary materials for the X-ray crystal structures of compounds Tpyb-Si, Tpyb-I, Mg(Tpyb-Si)$_2$ and Tpyb$_2$-FL. The data of bond lengths and bond angles are listed.

Crystal data and Structure Refinement details for Tpyb-Si, Tpyb-I, Mg(Tpyb-Si)$_2$ and Tpyb$_2$-FL.

Compound	Tpyb-Si	Tpyb-I	Mg(Tpyb-Si)$_2$	Tpyb$_2$-FL
empirical formula	$C_{24}H_{26}BN_3Si$	$C_{21}H_{17}BIN_3$	$3(C_{48}H_{50}B_2MgN_6Si_2)\cdot 5(C_6H_{12})$	$C_{55}H_{58}B_2N_6$
MW	395.38	449.09	2859.93	824.69
T, K	100(2)	100(2)	100(2)	100(2)
wavelength, Å	1.54178	1.54178	1.54178	1.54178
crystal system	Monoclinic	Monoclinic	Triclinic	Triclinic
space group	$P2_1$	$P2_1/n$	*P*-1	*P*-1
a, Å	11.2456 (2)	11.4562 (3)	9.2521 (6)	11.458 (2)
b, Å	7.2679 (1)	9.2595 (2)	19.3245 (13)	14.678 (2)
c, Å	14.5517 (3)	17.8090 (4)	24.5948 (17)	15.245 (3)
α, deg	90	90	100.575(4)	76.348(9)
β, deg	109.493(1)	97.476(1)	100.809(4)	70.761(8)
γ, deg	90	90	103.320(4)	73.177(8)
V, Å^3	1121.17 (3)	1873.10 (8)	4083.2 (5)	2288.9(7)
Z	2	4	1	2
ρ_{calc}, g cm^{-3}	1.171	1.592	1.163	1.197
μ (Cu Kα), mm^{-1}	1.02	13.49	1.02	10.13
crystal size, mm	0.20×0.12×0.05	0.33×0.27×0.20	0.25×0.18×0.11	0.27×0.25×0.11
θ range, deg	3.2-69.5	2.5-72.1	2.7-67.7	3.1-64.6
limiting indices	$-13\le h\le 13$	$-13\le h\le 14$	$-10\le h\le 10$	$-9\le h\le 10$
	$-8\le k\le 7$	$-11\le k\le 10$	$-21\le k\le 22$	$-13\le k\le 15$
	$-17\le l\le 16$	$-21\le l\le 21$	$-28\le l\le 28$	$-11\le l\le 15$
reflns collected	10329	8839	28214	5820
independent reflns	3704 [*R*(int) = 0.031]	3399 [*R*(int) = 0.043]	12505 [*R*(int) = 0.035]	3342 [*R*(int) = 0.050]
absorption correction	Numerical	Numerical	Numerical	Numerical
data/restraints/ parameters	3704 / 1 / 266	3399 / 0 / 236	12505 / 0 / 946	3342 / 0 / 571

goodness-of-fit on F^2	1.05	1.09	1.06	1.06
final *R* indices	$R1 = 0.037$	$R1 = 0.037$	$R1 = 0.067$	$R1 = 0.101$
[I >2σ(I)] [a]	w$R2 = 0.083$	w$R2 = 0.101$	w$R2 = 0.176$	w$R2 = 0.296$
R indices (all data) [a]	$R1 = 0.041$	$R1 = 0.038$	$R1 = 0.084$	$R1 = 0.110$
	w$R2 = 0.081$	w$R2 = 0.100$	w$R2 = 0.167$	w$R2 = 0.288$
$peak_{max}/hole_{min}$ (e Å^{-3})	0.24 / –0.21	1.18 / –1.63	0.72 / –0.45	0.67 / –0.55
Flack parameter	0.03(3)	–	–	–

Selected bond lengths [Å] and angles [º] for Tpyb-Si, Tpyb-I, Mg(Tpyb-Si)$_2$ and Tpyb$_2$-FL.

Compound	Tpyb-Si	Tpyb-I	Mg(Tpyb-Si)$_2$	Tpyb$_2$-FL
Mg-N			2.147(3)	
Mg-N			2.188(3)	
Mg-N			2.198(3)	
B-C(Ph)	1.637(3)	1.635(4)	1.646(5)	1.635(11)
B-C(Py)	1.625(3)	1.635(4)	1.643(6)	1.643(14)
B-C(Py)	1.634(3)	1.639(4)	1.658(6)	1.615(15)
B-C(Py)	1.639(3)	1.636(4)	1.660(5)	1.657(14)
N-C(B)	1.355(3)	1.362(4)	1.367(5)	1.373(11)
N-C(B)	1.362(3)	1.356(4)	1.370(4)	1.348(9)
N-C(B)	1.361(3)	1.355(4)	1.364(5)	1.363(10)
C(Py)-B-C(Ph)	108.44(17)	110.6(2)	112.7(3)	108.9(8)
C(Py)-B-C(Ph)	109.58(17)	110.1(2)	106.0(3)	108.8(7)
C(Py)-B-C(Ph)	110.90(17)	110.3(2)	114.5(3)	111.0(7)
C(Py)-B-C(Py)	111.37(17)	110.6(2)	102.4(3)	111.1(7)
C(Py)-B-C(Py)	107.26(17)	108.5(2)	110.1(3)	110.3(7)
C(Py)-B-C(Py)	109.28(17)	106.7(2)	111.3(3)	106.9(8)
N-Mg-N(trans)			175.91(12)	
N-Mg-N(trans)			175.66(13)	
N-Mg-N(trans)			179.18(13)	
N-Mg-N			95.77(13)	
N-Mg-N			96.90(13)	
N-Mg-N			91.69(12)	
N-Mg-N			90.16(12)	
N-Mg-N			92.52(12)	
N-Mg-N			94.83(13)	

Curriculum Vitae

SO YI JEONG
soyi.jeong@rutgers.edu

Date and Place of Birth

August 2nd, 1984, Seoul, South Korea

EDUCATION

Rutgers University, Newark, NJ, USA 2011– 2014
Master of Science in Chemistry
Advisor: Prof. Frieder Jäkle, Ph.D. (joint Project with Prof. John B. Sheridan, Ph.D.)

- GSGA Travel Award, Spring 2014
- Innovation Fellowship Program, Spring 2014

Kean University, Union, NJ, USA 2006 – 2010
Bachelor of Science in Chemistry
Minor in Mathematics
Supervisor: Prof. Matthew T. Mongelli, Ph.D. and Prof. Yeung G. Shin, Ph.D.

- Dean's List, Fall 2006

PRESENTATIONS

Jeong, S.Y.; Lupinska, P.; Cui, C.; Shipman, P. O.; Lalancette, R. A.; Sheridan, J. B.; Jäkle, F. "Second generation tris(2-pyridyl)borate ligands: toward supramolecular polymeric materials*"* ***Boron in the Americas (BORAM XIV),*** Newark, NJ, June 15-19, 2014. *Oral Presentation*

Jeong, S.Y.; Lupinska, P.; Cui, C.; Shipman, P. O.; Lalancette, R. A.; Sheridan, J. B.; Jäkle, F. "Second generation tris(2-pyridyl)borate ligands: toward supramolecular polymeric materials*"* ***247th ACS National Meeting***, Dallas, March 16-20, 2014. *Oral Presentation*

Jeong, S.Y.; Shipman, P. O.; Lalancette, R. A.; Sheridan, J. B.; Jäkle, F. "2nd generation tris(2-pyridyl)borate ligands: toward supramolecular polymeric materials*"* ***Graduate Poster Session***, Rutgers University, Newark, NJ, November 20, 2013. *Poster Presentation*

PROFESSIONAL EXPERIENCE

Research Scientist 2010 – 2011
Access Bio Inc., Somerset, NJ, USA

- Determination of Glucose-6-Phosphate Dehydrogenase(G6PD) enzyme activity in human blood
- Detection of Group A Streptococcal antigen directly from throat swab specimens